AJHG The American Journal of Human Genetics

# DNA methylation signature for EZH2 functionally classifies sequence variants in three PRC2 complex genes

--Manuscript Draft--

| | |
|---|---|
| **Manuscript Number:** | AJHG-D-19-00804R3 |
| **Full Title:** | DNA methylation signature for EZH2 functionally classifies sequence variants in three PRC2 complex genes |
| **Article Type:** | Article |
| **Keywords:** | EZH2; Weaver Syndrome; PRC2 complex; Overgrowth; DNA methylation; DNA methylation signature |
| **Corresponding Author:** | Rosanna Weksberg<br>[see notes]<br>Toronto, Ontario CANADA |
| **First Author:** | Sanaa Choufani |
| **Order of Authors:** | Sanaa Choufani |
| | William T. Gibson |
| | Andrei L. Turinsky |
| | Brian H.Y. Chung |
| | Tianren Wang |
| | Kopal Garg |
| | Alessandro Vitriolo |
| | Ana S.A. Cohen |
| | Sharri Cyrus |
| | Sarah Goodman |
| | Eric Chater-Diehl |
| | Jack Brzezinski |
| | Michael Brudno |
| | Luk Ho Ming |
| | Susan M. White |
| | Sally Ann Lynch |
| | Carol Clericuzio |
| | I Karen Temple |
| | Frances Flinter |
| | Vivienne McConnell |
| | Tom Cushing |
| | Lynne M. Bird |
| | Miranda Splitt |
| | Bronwyn Kerr |
| | Stephen W. Scherer |
| | Jerry Machado |
| | Eri Imagawa |
| | |

| | |
|---|---|
| | Nobuhiko Okamato |
| | Naomichi Matsumoto |
| | Guiseppe Testa |
| | Maria Iascone |
| | Romano Tenconi |
| | Oana Caluseriu |
| | Roberto Mendoza-Londono |
| | David Chitayat |
| | Cheryl Cytrynbaum |
| | Katrina Tatton-Brown |
| | Rosanna Weksberg |
| **Abstract:** | Weaver syndrome (WS), an overgrowth/intellectual disability syndrome (OGID), is caused by pathogenic variants in the histone methyltransferase EZH2 , a core component of the polycomb repressive complex-2 (PRC2). Using genome-wide DNA methylation (DNAm) data for 187 individuals with OGID and 969 controls, we show that pathogenic variants in EZH2 generate a highly specific and sensitive DNAm signature reflecting the phenotype of WS. This signature can be used to distinguish loss-of-function from gain-of-function missense variants , and to detect somatic mosaicism. We also show that the signature can accurately classify sequence variants in EED and SUZ12, encoding two other core components of PRC2, and predict the presence of pathogenic variants in undiagnosed individuals with OGID. The discovery of a functionally relevant signature with utility for diagnostic classification of sequence variants in EZH2, EED and SUZ12 supports the emerging paradigm shift for implementation of DNAm signatures into diagnostics and translational research. |

SickKids®
THE HOSPITAL FOR
SICK CHILDREN

UNIVERSITY
of TORONTO

March 05, 2020

Sarah Ratzel, PhD
Scientific Editor, AJHG

Sara Cullinan, PhD
Deputy Editor, AJHG

Bruce Korf, MD PhD
Editor, AJHG

Dear Drs. Ratzel, Cullinan and Korf:

We thank you for accepting our manuscript "**DNA methylation signature for *EZH2* functionally classifies sequence variants in three PRC2 complex genes**".

We have accepted all the changes, revised the affiliations and the acknowledgement and updated the data availability statement. In addition, we have revised Figure 1 to include HGVS-recommended nomenclature for protein change, updated reference 39 and updated the nomenclature and the font for the figures.

Sincerely yours,

R. Weksberg, MD, PhD, FRCPC, FCCMG, FACMG
Clinical Geneticist, Division of Clinical & Metabolic Genetics
Senior Associate Scientist, Research Institute
Hospital for Sick Children
Professor of Paediatrics and Genetics
Institute of Medical Science
University of Toronto
Phone: 416-813-6386
Fax: 416-813-5345
Email: rweksb@sickkids.ca

**Response to Reviewer's :**

**The response to the reviewer's are presented in bold.**

Reviewer #1: The Authors have addressed most of the issues raised in previous review and the manuscript is much improved.
I still feel the potential confound of blood cell type composition changes is only indirectly addressed (by computational methods) not by empirical validation; the Authors refer to previous work, referencing that blood cell type is not altered in WEAVER syndrome, but their study population is more broadly defined than Weaver.
Having said that, I understand it is simply not possible to properly study blood cell types in their complete cohort, so I would recommended to add a paragraph to the discussion section to briefly discuss potential limitations and confounds that might require follow-up in future work.

**Author Response: We thank the reviewer for his comment, and we have added the following to the discussion.**

**"In the development of DNAm signatures, an important consideration is the issue of cell type variation. As DNA methylation varies markedly among all cell types, including hematopoietic cells (Reinius et al., 2012), it is important to account for inter-individual differences in cell types of whole blood samples when analyzing DNAm data from this tissue (Jaffe and Irizarry, 2014). Here, we estimated the cell proportions in the discovery cohort using the Houseman method and included these estimates as covariates when identifying EZH2-specific signature. This method uses DNAm measured in purified blood cells from a small number of healthy adults to generate cell proportion estimates in mixed cell populations, such as whole blood. We found no statistically significant differences in blood cell type composition between the affected individuals and controls, which aligned with reports of individuals with EZH2-related overgrowth having typical blood cell composition (Genereviews reference Tatton-Brown). Future work measuring both complete blood counts and DNAm in the same individuals with WS is needed to confirm the efficacy of the Houseman method in this context."**

Reviewer #2:
Choufani and colleagues present a study in which they use DNA methylation patterns in peripheral blood leukocytes as a way of reporting the effects of mutations in genes involved in Polycomb silencing, EZH2, EED and SUZ12.
The rationale for this kind of approach has been presented previously by this and at least one other group - the assumption that genes with 'epigenetic' activities (modifying transcriptional regulators), when mutant, will cause cells to change their transcriptional regulatory profiles, which can be reported by DNA methylation as part of the cascade of resulting events.

Author action item:
* Please consider explaining the rationale for the study in terms like those used in the paragraph above. Coining words like 'epigenes' adds confusion on top of the ambiguity inherent to the use of words like 'epigenome' and 'epigenetic patterns of regulatory disruption', although the authors are credited for being more clear in the use of these terms than most.
The authors have convincingly demonstrated the power of this approach in prior studies of lysine methyltransferase (KMT2D) and lysine demethylase (KMT6D) mutations in Kabuki syndrome, and BAF-related mutations in Coffin-Siris and Nicolaides- Baraitser syndromes.
The authors now focus on genes encoding proteins in the Polycomb PRC2 complex, primarily looking at EZH2 mutations that cause the overgrowth/intellectual disability Weaver syndrome, which is inherited as an autosomal dominant disorder.
They collected well-characterised samples from both the phenotypic and the genetic perspectives. Their DNA methylation analysis looks to be appropriate.
Response: We thank the reviewer for the very positive comments and hope that our responses are acceptable. As suggested by the reviewer we have made some modifications to the rationale of the study. The following information has now been added to the Introduction: "We and others have recently found that disorders caused by pathogenic sequence variants in epigenes (genes encoding proteins that demonstrate "epigenetic" functions) may cause cells to change their typical DNA methylation and transcriptional profiles. Individuals with pathogenic variants in some epigenes exhibit disorder-specific signatures comprised of genome-wide, multilocus DNA methylation (DNAm) alterations. These signatures can be used to functionally classify sequence variants, with high sensitivity and specificity and to improve our understanding of the pathophysiology of the associated genetic disorder".
Reviewer response: While omitting the word 'epigenes' altogether would be far preferable, the edit is reasonable.

**Author Response: Thank you!**

Author action items:
A) While it seems appropriate to exclude the outlier sample from the PCA results, it would be instructive for others who may look to this study for guidance to have some forensic analysis of why the sample failed - poor quality or insufficient amount of DNA, a failed conversion/labelling/hybridization, sample swap, something else?
Response: We would like to clarify that only one outlier sample was identified in one dataset (GSE51245) of GEO control data. These data were downloaded to obtain additional control cohorts to demonstrate the high specificity of the EZH2 signature. This is documented in Table S7. The original IDAT files were not available for this specific dataset. Hence, we could only examine the pre-processed signal intensities per CpG available for this dataset and the resulting beta values. We observed an unusually large amount of very-high intensity CpGs in both unmethylated and methylated signals for the outlier sample GSM1240970. The distribution of

beta-values for GSM1240970 also looked markedly different from the other samples and also from the usual beta-value distributions obtained in such experiments. The low- and high-methylation peaks were much less pronounced and a much larger amount of off-peak CpGs were observed in the mid range of DNA methylation values. This likely resulted from flawed signal intensity inputs into the computation of the beta values for GSM1240970. These observations suggest that there were technical problems in the processing of this DNA sample which resulted in its classification as an outlier on PCA, and we therefore n removed it from our analysis. See the figure provided below. We have noted in Table S7 the exact accession number for the failed "control sample".
Reviewer response: Please add this information to the Supplement to demonstrate why the sample was omitted. It is useful guidance for others as well as giving insights into why your exclusion of the sample was justifiable.

**Author Response: This requested information has been added to the supplements as Figure S5.**

B) [line 196] 'Genome-wide DNAm profiling on control and affected subjects matched for tissue type,...' - wasn't there only one tissue type (blood) used?
Response: That is correct, the text was edited to reflect that only one tissue, blood, was used in this study.
C) The analysis involved adjustment for cell subtype composition, using the 6 blood cell subtypes reported by Houseman.
Author action item:
It's not clear why this was performed. The goal is to create a robust biomarker for the phenotype, isn't it? So if blood cell subtypes were to shift in proportions and generate a DNA methylation signal difference between the groups, that should only be helpful. Furthermore, if EZH2 mutations cause, for example, fewer CD8 cells, isn't that kind of interesting? I strongly urge the authors to review this aspect of the paper and (a) see if there is any evidence for cell subtype proportion changes associated with the mutations studied and, if so, (b) test whether the model works better by omitting the cell subtype proportion adjustment. I recognise that undertaking (b) could be taken to mean that the entire analysis in the manuscript would need to be repeated, which is unreasonable, so I suggest that if there is any evidence for improved prediction by including cell subtype variation, the authors can just make note that this could be an avenue for future improvement of the approach, it does not have to be included here.
Response: The blood cell proportions were estimated for the discovery set only using the Houseman method to allow cell type estimates to be included as covariates when identifying signature CpG sites. This approach is a common standard in DNA methylation analysis for blood -derived DNA to ensure that the identified significant CpG sites reflects true differences in DNA methylation between cases and controls that are not due to shifts in blood cell type proportions.

Given that we know that blood cell proportions are normal in individuals with Weaver syndrome, we were particularly interested in the molecular rather than cellular changes in Weaver patients. Our primary aim is to gain insights into the epigenetic mechanisms underlying this disorder. For Weaver syndrome, we found no statistically significant differences in blood cell type composition between the affected cases and controls (see our response to Reviewer 1's questions above). The robustness of the DNA methylation signature is presented in the validation cohort of Weaver patients with EZH2 mutations where no covariates were considered, i.e. sex, age, blood cell type proportions, when classifying these samples and the signature proved to be 100% sensitive and specific.

Our findings on the estimated cell type proportions in blood are in keeping with the current state of knowledge about these individuals i.e. individuals with EZH2- related overgrowth exhibit typical blood cell composition. (Genereviews reference Tatton-Brown; https://urldefense.proofpoint.com/v2/url?u=https-3A__www.ncbi.nlm.nih.gov_books_NBK148820_&d=DwIGaQ&c=Sj806OTFwmuG2UO1EEDr-2uZRzm2EPz39TfVBG2Km-o&r=51EKmW1yHhYfqz75880EyTnwCH0wOn1JwGd87xNaVZc&m=CQLSVTXTAlAiMggcLxnw3QXhO8d_EiA8--W0V7qPpWM&s=6I8mR59DBg2XdAO2s1KXobHQJki1enJMpnWYrhqFvy4&e= ; and personal communications Chitayat, Gibson, Tatton-Brown).

Reviewer response: I think we're talking at cross-purposes to some extent. The main point I wanted to make was that the test is defining a biomarker. As such, it doesn't matter whether the change in DNA methylation is due to cell subtype changes or not.  While the response to Reviewer 1 shows that there are no such cell subtype proportion changes detectable, the point I was trying to make was that if, for example, mutations of the polycomb genes systematically cause a decrease in CD8+ T cells in peripheral blood, incorporating this into the model (rather than excluding them analytically) would probably strengthen the performance of the biomarker. What the authors describe "This approach is a common standard in DNA methylation analysis for blood -derived DNA to ensure that the identified significant CpG sites reflects true differences in DNA methylation between cases and controls that are not due to shifts in blood cell type proportions" is only important when trying to gain mechanistic insights into cellular reprogramming.  That's a different goal from defining a robust biomarker.

There is nothing wrong with how the authors are responding to the point I've raised, it is just a point to consider for the future, not to get confused about supposed confounding influences in biomarker studies.

**Author Response: Thank you!**

D) The predictive model for EZH2 works very well, and was even able to identify, from a partially-predictive score, a case of mosaicism for an EZH2 mutation. In addition, a case with a de novo EZH2 variant was included and found to score in a way that put it into the control group, but was found to have changes of DNA methylation opposite to those of the other EZH2

mutations. It raised interest because "it generated a DNAm profile opposite to that of the WS cases and very different from control individuals". While the heatmap of Figure 5A is meant to show us this opposite pattern, that's not really clear. By definition, the controls should have this opposite pattern.
Author action item:
What needs to be illustrated somehow is that this case, across multiple loci, has a pattern that has a DNA methylation change that is not only in the same direction as the controls, not the other EZH2 cases, it exceeds the typical range for controls in that direction.
Response: This is a great suggestion. Figure S2 has been added to better illustrate the findings.
Reviewer response: Impressive figure. Glad the suggestion was useful.

**Author Response: Thank you!**

D) The biochemical testing to demonstrate the gain of function of this mutation is really compelling. However, the assumption that a gain of function mutation should change DNA methylation in the opposite direction to a loss of function mutation is very interesting, but the speculation about this finding in the Discussion [lines 593-606] are problematic. The statement that "EZH2-mediated H3K27 methylation can modulate CpG methylation" is uncited, and this is a difficult area to understand from the biochemical perspective, much of the work in this field dating from ~2006-2007. It does not seem reasonable to claim that the authors' "discovery suggests a possible mechanism for epigenetic memory in which an 'epigenetic memory module' consisting of both EZH2 and DNMTs could coordinate the heritable transmission of silenced epigenetic states through various rounds of post-zygotic DNA replication", as the mutation is present both before and after replication, the DNA methylation change can be established anew at each round of replication. Furthermore, the prior work on NSD1 does not show the "transgenerational transmission of specific DNAm states" - looking at that paper, there was no study of multiple generations, this is a bizarre and sensational statement. The authors are not studying the transmission of DNA methylation states as if they are independently self-propagating themselves, they are studying DNA mutations that are being passed from parent to daughter cells, leading to DNA methylation changes somehow.
Response: As suggested by this reviewer we have removed all references to epigenetic memory and transgenerational inheritance.
With respect to the NSD1 paper (Choufani et al, 2015), we presented data for a two-generation family with one father and two affected siblings (DI50448; DL50450 and DL50452 are the individual IDs as presented in Table S1 of the NSD1 paper). All three shared the same NSD1-specific DNA methylation signature as shown for the EZH2-siganture in the current manuscript. This is an extract from the method of the NSD1 paper under "Differential DNA methylation analysis" section. "To identify the differentially methylated CpG sites, we compared the DNAm distributions for Sotos cases versus controls at each CpG site. To account for the influence of the family relationships among three of the SS patients, we formed three separate testing trials,

each time combining 16 non-familial Sotos cases with only one family member...."
Reviewer response: Removal of the statements addresses the concern.

**Author Response: Thank you!**

E) The authors have made a very interesting observation about loss and gain of function mutations of EZH2 and associations with DNA methylation changes. More discussion to put this into the context of what is known about PRC2-DNA methylation regulation would be valuable.
Response: We agree with the reviewer that further discussion regarding the mechanism of PRC2 -DNA methylation regulation would benefit the manuscript. The following text has been added to the discussion. "PRC2 belongs to the Polycomb group (PcG) proteins family of chromatin-modifying enzymes that function as repressors of gene expression (Schuettengruber et, al 2017). In mammalian cells, PRC2 is primarily targeted to the unmethylated CpG islands of inactive developmental genes (Li et al, 2017). PRC2 recruitment and binding to the targeted CpG island is facilitated in part by polycomb-like proteins (PCLs) and JARID2 which link the PRC2 complex to genomic sites enriched in CpG dense regions (Li et al, 2017; Youmans et al 2018). In the EZH2 LoF (hypomorphic) state, we observed a loss of DNA methylation at CpG sites enriched in promoter regions of developmental genes which can lead to transcriptional changes during critical developmental timepoints resulting in somatic overgrowth characteristic of WS. In the case of the EZH2 GoF state, we observed a gain of methylation at the same CpG sites which can lead to transcriptional changes during development resulting in growth restriction. Further work is needed to explore the underlying transcriptional dysregulation at the gene promoters overlapping the EZH2-specific signature in relevant cell types and critical timepoints during development."
Reviewer response:  That seems like a reasonable discussion of this interesting finding.

**Author Response: Thank you!**

F) Unfounded statements ("EZH2-mediated H3K27 methylation can modulate CpG methylation", "discovery suggests a possible mechanism for epigenetic memory in which an 'epigenetic memory module' consisting of both EZH2 and DNMTs could coordinate the heritable transmission of silenced epigenetic states through various rounds of post-zygotic DNA replication", "transgenerational transmission of specific DNAm states") need to be eliminated and replaced with more temperate and precise language. For example, "transgenerational" has a common meaning in the field of epigenetics (PMID: 17949945). More precise description of what the authors are trying to communicate would be very helpful.
Response: We thank the reviewer for his/her comments, and we have clarified the discussion to reflect our findings.
"Our results support the position that the DNA methylation changes observed in individuals carrying germline EZH2 pathogenic variants represent a downstream cascade of events at the molecular level in response to a genetic change. These DNA methylation changes recur across

multiple generations if the genetic change is present demonstrating the impact of EZH2 pathogenic variants on epigenetic programming during embryonic development".
Reviewer response:  This is much more clear and accurate, good response.

**Author Response: Thank you!**

G) The value of this approach to understand the effects of DNA sequence variants, the detection of somatic mosaicism, the commonalities between phenotypes caused by mutations in different genes, the differences in phenotypes caused by different types of mutations in the same gene, and the ability to understand phenotypic heterogeneity is really compelling. This is a really nice study and an excellent contribution to the field.
Response: We thank the reviewer for highlighting the important contribution of the study to the field.
Minor edits:
*       *  [line 263] consequitive -Corrected
*       *  [line 337] subjects- This refers to other protein members of the PRC2 complex, therefore not corrected
Reviewer response:  Now line 344, the sentence starts with lower case "subjects that were identifiedâ□¦", not sure how that can have been missed repeatedly.
**Author Response: Fixed**

*       * [line 345] ;-Not clear what the reviewer is referring to.
Reviewer response:  Now line 352, the semicolon is followed by a capitalised word and what appears to be a new sentence, so a period seems more appropriate.

**Author Response: Fixed**

# DNA methylation signature for *EZH2* functionally classifies sequence variants in three PRC2 complex genes

Sanaa Choufani,[1] William T Gibson,[2] Andrei L. Turinsky,[1,3] Brian H.Y. Chung,[4] Tianren Wang,[1] Kopal Garg,[1] Alessandro Vitriolo,[5] Ana S.A. Cohen,[2,6] Sharri Cyrus,[2] Sarah Goodman,[1] Eric Chater-Diehl,[1] Jack Brzezinski,[1,7] Michael Brudno,[1,3,8] Luk Ho Ming,[9] Susan M. White,[10] Sally Ann Lynch,[11] Carol Clericuzio,[12] I Karen Temple,[13] Frances Flinter,[14] Vivienne McConnell,[15] Tom Cushing,[16] Lynne M. Bird,[17] Miranda Splitt,[18] Bronwyn Kerr,[19] Stephen W. Scherer,[1,20] Jerry Machado,[21] Eri Imagawa,[22] Nobuhiko Okamoto,[23] Naomichi Matsumoto,[22] Guiseppe Testa, [5, 24] Maria Iascone,[25] Romano Tenconi,[26] Oana Caluseriu,[27] Roberto Mendoza-Londono,[28, 29] David Chitayat,[28, 29,30] Cheryl Cytrynbaum,[1,28,31] Katrina Tatton-Brown,[32] and Rosanna Weksberg[1,28,29,31,33]*

1) Genetics and Genome Biology, The Hospital for Sick Children, Toronto, Ontario M5G 1X8, Canada.
2) British Columbia Children's Hospital Research Institute, Vancouver, BC V5Z 4H4, Canada. Department of Medical Genetics, University of British Columbia, Vancouver, BC V6H 3N1, Canada.
3) Centre for Computational Medicine, The Hospital for Sick Children, Toronto, Ontario M5G 1X8, Canada.
4) Pediatrics and Adolescent Medicine, Queen Mary Hospital and Hong Kong Children's Hospital, The University of Hong Kong, 999077 Hong Kong.
5) Department of Oncology and Hemato-oncology, University of Milan, Milan 20122, Italy; Laboratory of Stem Cell Epigenetics, IEO, European Institute of Oncology, IRCCS, Milan 20139, Italy.
6) Department of Genetics and Genomic Sciences, Icahn School of Medicine at Mount Sinai, New York, NY 10029, USA.
7) Division of Haematology and Oncology, The Hospital for Sick Children, Toronto, Ontario, M5G 1X8 Canada; Department of Pediatrics, University of Toronto, Toronto, Ontario, M5G 1X8 Canada.
8) Department of Computer Science, University of Toronto, Toronto, Ontario, M5S 3H5, Canada.
9) Clinical genetic service, Department of Health, 999077 Hong Kong.
10) Victorian Clinical Genetics Service, Murdoch Children’s Research Institute, Melbourne 3052, Australia; Department of Paediatrics, University of Melbourne, Melbourne 3052, Australia.
11) Department of Clinical Genetics, Temple Street Children's University Hospital, Dublin, D01 XD99, Ireland.

12) Pediatric Genetics, University of New Mexico, Albuquerque, New Mexico 87131, USA.
13) Faculty of Medicine, University of Southampton and the Wessex Clinical Genetics Service, University Hospital Southampton NHS Foundation Trust, Southampton SO16 6YD, UK.
14) Department of Clinical Genetics, Guy's and St Thomas' NHS Foundation Trust, London SE1 9RT, UK.
15) Northern Ireland Regional Genetics Service, Belfast City Hospital, Belfast BT9 7AB, UK.
16) Pediatric Genetics, University of New Mexico, Albuquerque, New Mexico 87131, USA.
17) Department of Pediatrics, University of California, San Diego, San Diego, CA 92093, USA; Division of Genetics, Rady Children's Hospital of San Diego, San Diego, CA 92123, USA.
18) Northern Genetics Service, Institute of Genetics Medicine, Newcastle upon Tyne NE1 3BZ, UK.
19) Division of Evolution and Genomic Sciences, School of Biological Sciences, University of Manchester, Manchester M13 9PL, UK; Manchester Centre for Genomic Medicine, Manchester University Hospitals NHS Foundation Trust, Manchester Academic Health Sciences Centre, Manchester M13 9WL, UK.
20) Department of Molecular Genetics, University of Toronto, Toronto, Ontario, M5S 1A1, Canada; The Centre for Applied Genomics, The Hospital for Sick Children, Toronto, Ontario M5G 1X8 Canada; McLaughlin Centre, University of Toronto, Toronto, Ontario, M5S 1A1, Canada.
21) PreventionGenetics, Marshfield, WI, 54449, USA.
22) Department of Human Genetics, Yokohama City University Graduate School of Medicine, Fukuura 3-9, Kanazawa-ku, Yokohama, 236-0004, Japan.
23) Department of Medical Genetics, Osaka Medical Center and Research Institute for Maternal and Child Health, Osaka 594-1101, Japan.
24) Human Technopole, Center for Neurogenomics, Via Cristina Belgioioso 171, Milan 20157, Italy.
25) Laboratorio di Genetica Medica, ASST Papa Giovanni XXIII, Piazza OMS 1, 24127 Bergamo, Italy.
26) Dipartimento Pediatria, University of Padova, Via Giustiani 3, 35128, Padova, Italy
27) Department of Medical Genetics, University of Alberta, Edmonton, AB, T6G 2H7, Canada; The Stollery Pediatric Hospital, Edmonton, AB, T6G 2H7, Canada.
28) Division of Clinical and Metabolic Genetics, The Hospital for Sick Children, Toronto, Ontario M5G 1X8, Canada.
29) Department of Pediatrics, University of Toronto, Toronto, Ontario, M5S 1A1, Canada.
30) Prenatal Diagnosis and Medical Genetics Program, Mount Sinai Hospital, Toronto, Ontario, M5G 1X5, Canada.
31) Department of Molecular Genetics, University of Toronto, Toronto, Ontario, M5S 1A1, Canada.
32) St George's University Hospitals NHS Foundation Trust, London SW17 0QT, UK; St George's, University of London, London SW17 0RE, UK; Section of Cancer Genetics, Institute of Cancer Research, Surrey SM2 5NG, UK.
33) Institute of Medical Sciences, University of Toronto, Toronto, Ontario M5S 1A8, Canada.

*Correspondence: rweksb@sickkids.ca

## Abstract

Weaver syndrome (WS), an overgrowth/intellectual disability syndrome (OGID), is caused by pathogenic variants in the histone methyltransferase *EZH2*, a core component of the Polycomb repressive complex-2 (PRC2). Using genome-wide DNA methylation (DNAm) data for 187 individuals with OGID and 969 controls, we show that pathogenic variants in *EZH2* generate a highly specific and sensitive DNAm signature reflecting the phenotype of WS. This signature can be used to distinguish loss-of-function from gain-of-function missense variants, and to detect somatic mosaicism. We also show that the signature can accurately classify sequence variants in *EED* and *SUZ12*, encoding two other core components of PRC2, and predict the presence of pathogenic variants in undiagnosed individuals with OGID. The discovery of a functionally relevant signature with utility for diagnostic classification of sequence variants in *EZH2, EED* and *SUZ12* supports the emerging paradigm shift for implementation of DNAm signatures into diagnostics and translational research.

## Introduction

Weaver syndrome (WS [MIM: 277590]), an overgrowth/intellectual disability syndrome (OGID), is characterized by pre- and postnatal overgrowth, accelerated osseous maturation, characteristic craniofacial features and variable intellect.[1] Sequence variants in *EZH2* (Enhancer of Zeste, drosophila, homolog 2 [MIM: 601573]) are the primary reported cause of WS, [2; 3] accounting for more than 90% of individuals. *EZH2* encodes part of the catalytic component of the polycomb repressive complex 2 (PRC2), which regulates genome-wide chromatin structure and gene expression through methylation of lysine 27 of histone H3; this mark drives chromatin condensation and transcriptional repression. [4] EZH2 in combination with EED (Embryonic Ectoderm Development [MIM: 605984]) and SUZ12 (SUZ12 polycomb repressive complex 2 subunit [MIM: 606245]) form the core complex of PRC2. Recently, it has been established that pathogenic variants in *EED* and *SUZ12* cause two clinically overlapping OGID syndromes, Cohen-Gibson (MIM: 617561) and SUZ12-related overgrowth syndrome, respectively. [5; 6]

The phenotypic consequences of pathogenic variants in *EZH2* are variable; clinical diagnosis is therefore challenging in the absence of the characteristic facial phenotype. The clinical features can be age dependent, and in the largest case series to date, fewer than half (47%) of individuals with *EZH2* pathogenic variants were considered to have the classic Weaver syndrome facial gestalt.[1] Tall stature, with a height at least two standard deviations (SDs) above the mean, is the most consistent EZH2-related clinical feature, present in ~90% of affected individuals. Intellectual disability is also common, present in ~80%, but can be very mild. However, tall stature and intellectual disability are nonspecific and generally common, which limits their utility as discriminating clinical features of WS and its related disorders. [1]

Several studies have shown that WS-associated pathogenic *EZH2* variants cause a loss rather than a gain of enzymatic activity. Cohen *et al.* [7] found reduced histone methyltransferase activity using an *in vitro* assay. In a mouse model of WS, decreased di- and trimethyl-H3K27 were identified in homozygous and heterozygous embryos, thereby supporting a role for reduced methyltransferase function as the cause of WS. [8]

We and others have recently found that disorders caused by pathogenic sequence variants in epigenes (genes encoding proteins that demonstrate "epigenetic" functions) may cause cells to change their typical DNA methylation (DNAm) and transcriptional profiles. Individuals with pathogenic variants in some epigenes exhibit disorder-specific signatures comprised of genome-wide, multilocus DNA methylation alterations. These signatures can be used to functionally classify sequence variants, with high sensitivity and specificity and to improve our understanding of the pathophysiology of the associated genetic disorder. [9-15] We have also shown that pathogenic sequence variants in clinically overlapping, genetically distinct disorders may lead to similar epigenetic patterns of regulatory disruption. Our group has recently reported this phenomenon in Kabuki syndrome (KS) types 1 and 2,  for which sequence variants in different causative genes (*KMT2D* [MIM: 602113] , *KDM6A* [MIM: 300128] ) share an epigenetic disease signature [10] and in BAF complex-associated disorders, we and others have reported similar findings. [12; 15]

In this study, we identified a genome-wide DNAm signature associated with pathogenic variants in *EZH2*. We were successful in using this signature to detect somatic mosaicism for *EZH2* variants and to classify both gain-of-function (GoF) and loss-of-function (LoF or hypomorphic) sequence variants in *EZH2*. Further, this *EZH2* signature can be used to identify and classify pathogenic sequence variants in other genes in the PRC2 core complex, namely

*EED* and *SUZ12*. These data provide the first evidence for convergent molecular signatures for three PRC2 complex genes and highlight the functional relevance of this DNAm signature for predicting variant pathogenicity, detecting somatic mosaicism, and most importantly, for discriminating different functional effects of sequence variants.

## Subjects and Methods

### Cohort with *EZH2* variants

The research was approved by the Research Ethics board at The Hospital for Sick Children (REB# 1000038847) and consent was obtained from participating subjects and /or their parents or guardians. Peripheral blood samples from subjects with *EZH2* variants (n=40) were used in this study, of whom eight unrelated subjects were used as a discovery set with a clinical diagnosis of Weaver syndrome and pathogenic sequence variants in *EZH2,* seven previously published in [2; 7] and one unpublished case (see Table S1). Another unrelated cohort with clinical diagnosis of WS consisting of eight previously published WS individuals with pathogenic *EZH2* sequence variant as part of the Childhood Overgrowth Consortium in the UK[1] was used as an independent validation set (Table S2). This *EZH2* variant cohort included a familial case series with a pathogenic *EZH2* sequence variant: GenBank: NM_004456.4; c.466A>G [p.Lys156Glu]. The proband has a family history of overgrowth, and the *EZH2* sequence variant segregated with the overgrowth phenotype over three generations. The family included the proband, two affected siblings, the mother and maternal grandfather. [3] An additional test cohort for *EZH2* variant classification consisted of 19 samples with *EZH2* variants (see Table S9), collected from PreventionGenetics, USA; from British Columbia Children’s Hospital at the University of British Columbia, Vancouver, Canada; from St George's University Hospitals NHS Foundation Trust, London, UK; from the Department of Human Genetics, Yokohama City University

Graduate School of Medicine, Fukuura, Japan; from Laboratorio di Genetica Medica, ASST Papa Giovanni XXIII, Piazza OMS, Bergamo, Italy; from the Department of Medical Genetics, University of Alberta, Edmonton, Canada; and from the Victorian Clinical Genetics Services, Murdoch Children's Research Institute, Royal Children Hospital, Victoria , Australia

### Cohort with *EED* variants

Three individuals with *de novo EED* pathogenic variants were previously reported[5-7] and are described in Table S9.

### Cohort with *SUZ12* variants

Five individuals with *SUZ12* variants were recruited to the study including one previously reported familial case comprised of the proband and affected father. [6] Two individuals with missense variants in *SUZ12* recruited from British Columbia Children's Hospital at the University of British Columbia, Vancouver, Canada and from the Department of Pediatrics and Adolescent Medicine from the University of Hong Kong. One autism case with 17q11.2 dup overlapping *SUZ12* identified at the Hospital for Sick Children, Toronto, Canada. Full description of the sequence variants is given in Table S9.

All gene variant annotations as well as *in silico* prediction using PolyPhen-2, SIFT, and MutationTaster were generated using Alamut visual 2.11. CADD scores were obtained using CADD database v1.4.

### Control Cohort

Genomic DNA from peripheral blood was obtained on a set of controls (n=23) selected as age- and sex- matched neurotypical controls to the *EZH2* discovery set (Table S3). In addition, 148 controls were used to determine the specificity of the DNAm signature. These control samples were obtained from the POND Network, The Hospital for Sick Children, and The University of Michigan (Dr. Greg Hanna).[16] Neurotypical was defined as healthy and developmentally normal on formal cognitive/behavioral assessments (samples from POND and The University of Michigan) or via physician/parental screening questionnaires (Hospital for Sick Children). Additional blood controls were obtained from publicly available datasets taken from the Gene Expression Omnibus. In total,

we used data from 718 unrelated subjects from the general population without clinically-obvious neurodevelopmental phenotypes, who had DNA extracted from peripheral blood and had undergone profiling with the Illumina 450k array (GSE54670, GSE54399, GSE51245, GSE89353, GSE36064, GSE128801, GSE53045, GSE40279, GSE42861).[17-25] We restricted subjects to those age <50 years to match our Weaver cohort and excluded one control sample, as it presented as outlier based on principal component analysis (PCA) of autosomal probes. For detailed information see Table S7 and Figure S5.

## DNAm array processing

Genome-wide DNAm profiling on control and affected subjects matched for age and sex was performed at The Center for Applied Genomics (TCAG), SickKids Research Institute, Toronto, Ontario, Canada. Genomic DNA from each subject was sodium bisulfite converted using the EpiTect Bisulfite Kit (EpiTect PLUSBisulfite Kit, QIAGEN, Valencia, CA), according to the manufacturer's protocol. Modified genomic DNA was then processed and analyzed on the Infinium HumanMethylationEPIC BeadChip (Illumina 850K) according to the manufacturer's protocol.[26] The distribution of the samples on the arrays was randomized for both disease and control samples. All signature-derivation samples (WS and controls) were run in the same batch.

*Quality control and normalization*: The raw IDAT files were converted into β-values, which represent DNAm levels as a percentage (between 0 and 1), using the *minfi* Bioconductor package in *R*. Data preprocessing included filtering out non-specific probes (41,135 probes); probes with detection p-value > 0.05 in more than 25% of the samples (824 probes); probes with single nucleotide polymorphic sites (SNPs) located within 10 bp of the targeted CpG site or a single base extension as well as probes near SNPs with minor allele frequencies above 1% (n=29,958); probes with raw beta = 0 or 1 in > 0.25 % of samples (n=21); non-CpG probes (n=2,932); and X and Y chromosome probes (n=19,627) for a total of 91,343 probes removed and a total of n=774,516 probes remaining for differential methylation analysis. Standard quality control metrics in *minfi* were used, including median intensity QC plots, density plots, and control probe plots: all samples passed quality control and were included in the study.

## Differential DNAm analysis

The analysis was performed using our previously published protocol. [10] Differential DNAm analysis between WS and controls was performed at 774,516 CpG sites using beta scores, which represent DNAm levels as a percentage (between 0 and 1). The β-value from each sample at the remaining 774,516 CpGs was used for downstream analysis and generation of a DNAm signature. Beta values were logit transformed to M-values using the following equation: log2(beta/(1-beta)). A linear regression modeling using *limma* package [27] was used to identify the differentially methylated probes. We estimated blood cell proportions using Houseman's algorithm and the Bioconductor packages, *minfi* and *FlowSorted.Blood.EPIC*. This method generates proportions of CD8+ T cells, CD4+ T, natural killer, B cells, monocytes and granulocytes (mainly neutrophils, Neu) (Table S13).[28] These estimated values for each cell component were incorporated into the model matrix of the regression analysis as covariates along with sex and age . The analysis was done on the discovery set of eight WS and 23 controls per the following regression model: DNAm was regressed against sex+age+ CD8T+CD4T+NK+Bcell+Mono+Neu for each CpG site. The generated *p*-values were corrected for multiple testing using the Benjamini-Hochberg method. A significant difference in DNAm between WS and control samples for each CpG site was required to meet the cutoffs of Benjamini-Hochberg adjusted *p*-values<0.05 and $|\Delta\beta| \geq 0.10$ (10% methylation differences) as previously reported [9; 10] .

## Generation of disease score classification model using correlation analysis

We used a previously described pipeline for generating disease scores using an established disease-specific DNAm signature. [9; 10] At each of the 229 signature CpGs, a median DNAm level was computed across the WS individuals (n=8) used to generate the signature, resulting in a reference profile. Similarly, a robust median-DNAm reference profile for the signature controls (n=23) was created. The classification of each additional gene variant or control DNAm sample was based on extracting a vector *B*R$_{sig}$R of its DNAm values in the signature CpGs and comparing *B*R$_{sig}$R to the two reference profiles computed above. *EZH2* score was defined as: *EZH2 score = r(B*R$_{sig}$R*, WS profile) – r(B*R$_{sig}$R*, control profile))* where *r* is the Pearson correlation coefficient. A classification model was developed based on scoring each new DNAm sample using the *EZH2* Score: a test sample with a positive score is more similar to the WS reference profile based on the signature CpGs and is therefore classified as “pathogenic”; whereas a sample with a negative score is more similar to the control-blood reference profile and is classified as “benign”. The classification is implemented in *R*. To test specificity, EPIC array data from 148 additional neurotypical controls were scored and classified. To test sensitivity, eight additional unrelated WS individuals with *EZH2* pathogenic variants were scored and classified.

### Generation of machine learning model for variant classification

Using the R package caret, probes with very similar methylation patterns with correlation greater or equal to 90% (redundant probes) were removed as we previously described [10] leading to a subset of 119 CpGs. Next, we developed a machine-learning model, a support vector machine (SVM) model with linear kernel that had been trained on the significant CpG sites from the discovery cohorts after further filtering to remove redundant CpGs. The model was set to the "probability" mode to generate SVM scores ranging between 0 and 1 (or 0 and 100%), thus classifying samples as "WS" (high scores) or "not-WS" (low scores). This SVM model was built as a tool for the classification of variants in *EZH2*, *EED* and *SUZ12*.

### Identification of differentially methylated regions

To identify differentially-methylated regions (DMRs) that are associated with *EZH2* variants, we used the bumphunting method[29] which strengthens the detection of regional differences by combining differential-methylation patterns across neighboring CpG sites. [30] The bumphunting design matrix accounted for the potential confounding effects of sex and age and was used to identify regions with consecutive CpGs no more than 0.5 Kb apart and an average regional methylation difference $|\Delta\beta|\geq 10\%$. Statistical significance was established using 1,000 randomized bootstrap iterations, as is recommended in the Bioconductor *bumphunter* package when accounting for confounders. The resulting DMRs were post-filtered to retain only those with *p*-value<0.05 and a length (number of consecutive CpGs) of at least five CpGs. The analysis was performed on the same sets of cases and controls used as the discovery cohort.

### Genomic and gene-set enrichment analyses

For genomic enrichment analysis, the list of 229 CpG sites (foreground genomic regions) was submitted to GREAT (Genomic Regions Enrichment of Annotations Tool) [31] using the default settings. We used the set of CpG sites after *minfi* probe quality control (n=774,516) as the background genomic regions.

Gene-set enrichment analysis was performed using g: Profiler to identify Gene Ontology (GO) Biological Process terms overrepresented in the annotations of genes overlapping the differentially methylated CpGs. The enriched GO terms with Benjamini-Hochberg corrected p-values <0.05 were reported. The redundant GO terms were reduced and visualized as interactive networks using EnrichmentMap app on the Cytoscape platform as previously described. [32]

### Enzymatic activity of EZH2

The luminescence assay to determine EZH2 enzymatic activity for the p.Ala738Thr sequence variant was performed at BPS Bioscience as follows: a 50 ul reaction mix containing 50 uM S-adenosylmethionine, EZH2 enzyme (as part of an artificially-assembled PRC2 complex derived from baculovirus expression vectors), and 20 mM phosphate buffer pH 7.4, 0.05% Tween-20 HMT buffer 2 (BPS #52170) was added to wells coated with the substrate. Incubation was done for one hour at room temperature, then antibody against methylated lysine 27 (K27) residue of histone H3 was added and incubated for one hour. Secondary horseradish peroxidase (HRP)-labeled antibody was added and incubated for 30 min. Finally, HRP chemiluminescent substrates were added and luminescence was read in using a microplate chemiluminescence reader. Control replicates were done with two different lot numbers of baculovirus-expressed human EZH2 bearing the canonical protein sequence, and a third iteration of the assay was done with EZH2 bearing a Threonine residue at position 738, replacing the Alanine.

## Molecular Protein Modeling

We applied PRODRG [33]- a tool for high-throughput crystallography of protein-ligand complexes. to build ad hoc topologies of S-Adenosyl methionine (SAM) and S-Adenosyl homocysteine residues for Gromacs. We performed homology modeling via Modeller v 9.22, [34] setting the MD refinement value to "refine.very_slow" and leaving the remaining parameters at default. Only the SET and post-SET domains of EZH2 were modelled to conform with i) the absence of known structures for the post-SET domain and ii) the need to simplify the model also in terms of computational costs and complexity. As a template structure for the modeling of SET domain we used 4MI0 [35].

*Energy Minimization and ΔG measurements:* Potential Energy minimization was performed on each EZH/SAH complex structures with GROMACS 2019 through a multi-step conjugate gradient algorithm using Amber99-ILDN force-field [36]. The minimization procedure automatically stopped when the resulting structure reached an RMSD threshold of 0.01. Estimates of the Free Energy of binding of each complex was measured via autodockVina. [37]

## Screening of subjects affected by syndromic overgrowth

We tested the DNAm signature generated for *EZH2* against DNAm profiles generated on other syndromic overgrowth cohorts including subjects with Sotos syndrome and pathogenic variants in *NSD1* (n=49),[9] Tatton-Brown Rahman syndrome and pathogenic variants in *DMNT3A* (n=5) [22] and susceptibility to autism and pathogenic variants in *CHD8* (n=10).[14] DNAm profiles at the 229 CpG sites were extracted from each subject and tested using the disease score correlation matrix against the DNAm profiles of controls and WS. DNAm profiles for all these subjects were generated on the Illumina 450k array.

**Cohort with undiagnosed overgrowth and intellectual disability**

Samples with undiagnosed overgrowth and intellectual disability who had tested negative for *NSD1* and/or *EZH2* coding variants were included in this analysis. These samples were profiled on the Illumina 450k array as part of a large cohort study of overgrowth syndromes at the Weksberg lab with samples collected from the division of Clinical Genetics at The Hospital for Sick Children, at the Department of Pediatrics and Adolescent Medicine from the University of Hong Kong, and at British Columbia Children's Hospital at the University of British Columbia. The UBC study recruited some samples referred in by international collaborators, some of which were referred because of a known variant in *EZH2*, and others referred in for the purposes of identifying the cause of undiagnosed overgrowth and/or intellectual disability. Samples included 73 DNAm profiles from blood-derived DNA generated on the Illumina 450k array. DNAm profiles at the *EZH2*-specific classification signature were extracted from each subject and tested using the disease score classification model to establish diagnosis in a search of potential individuals with WS. Once a DNAm profile similar to WS was identified in these undiagnosed individuals, next-generation sequencing was performed on these individuals to identify variants in PRC2 complex members.

## Whole genome sequencing

Subjects that were identified with DNAm profiles similar to the WS profile were subjected to next-generation sequencing for variant identification. About 1 ug of genomic DNA was submitted to TCAG for genomic library preparation and whole genome sequencing. DNA samples were quantified using Qubit High Sensitivity Assay and sample purity was checked using Nanodrop OD260/280 ratio. Seven hundred ng of DNA was used as input material for library preparation using the Illumina TruSeq PCR-free DNA Library Prep Kit following the manufacturer's recommended protocol. In brief, DNA was fragmented to an average size of 400 bp using sonication on a Covaris LE220 instrument; fragmented DNA was end-repaired, A-tailed and indexed TruSeq Illumina adapters with overhang-Ts added to the DNA. Libraries were validated on a Bioanalyzer DNA High-Sensitivity chip to check for size and absence of primer dimers and quantified by qPCR using the Kapa Library Quantification Illumina/ABI Prism Kit protocol (KAPA Biosystems). The Validated library was paired-end sequenced on the Illumina HiSeq X platform following Illumina's recommended protocol to generate paired-end reads of 150-bases in length.

## Pyrosequencing

Genotyping was performed using quantitative pyrosequencing for *EZH2* variant: GenBank: NM_004456.4; c.2006G>A [p.Ser669Asn] in a father-child pair. Targeted assay was designed using the PyroMark Assay Design Software 2.0 (Qiagen). Primer set sequences consisted of forward primer-5'-AAGCTGACAGAAGAGGGAAAGTG; reverse primer 5'-TCCCAGCTCTGAAACATACCA  and sequencing primer 5'-TTCAAGTTGAACAGAAAG.

The amplification protocol was developed using a biotinylated universal primer approach. Regions of interest were amplified by PCR and pyrosequencing was carried out using the PyroMark Q24 pyrosequencer (Qiagen) according to the manufacturer's protocol. Output data were analyzed using PyroMark Q24 Software (Qiagen), which calculates the allelic percentage for each allele, allowing quantitative comparisons.

### Ethics Statement

The study protocol has been approved by the Hospital for Sick Children Research Ethics Board (REB 1000038847). All the participants provided informed consent prior to sample collection. All samples and records were de-identified before any experimental or analytical procedures. The research was conducted in accordance with all relevant ethical regulations.

## Results

### Identification of DNAm signature in Weaver syndrome

To identify an *EZH2* DNAm signature, we generated genome-wide DNAm profiles using Infinium HumanMethylationEPIC BeadChip arrays to test DNA from blood samples of individuals with pathogenic sequence variants in *EZH2* and controls. A comprehensive map illustrating the specific variants in *EZH2* and the number of affected individuals for each variant is shown in Figure 1. The complete WS cohort included 21 subjects, all of whom had clinical features of WS and *EZH2* pathogenic sequence variants identified in molecular diagnostic laboratories (Tables S1 and S2). The Canadian cohort was used for discovery (n=8 unrelated individuals) (Table S1) and the UK cohort was used for validation (n=8 unrelated subjects and n=5 affected members of the same family) (Table S2). Both cohorts included individuals from international centers. The demographics for the discovery cohort were as follows: for WS there were five males and three females and the mean age ± standard deviation at sample collection was 16 ± 14.7 years (range 1–43 years). The 23 sex- and age-matched control subjects included 15 males and eight females; their mean age at the time of sample collection was 15.9 ± 9.8 years (range 3-39 years) (Table S3).

We used our established pipeline as outlined in the Methods for signature derivation. Of the 774,516 CpG sites tested for differential DNAm between WS and controls, we identified 229 statistically significant changes in DNAm across the genome at an FDR adjusted *p*-value<0.05 and $|\Delta\beta| \geq 0.10$ (Table S4). Over 81% of these sites showed hypomethylation in WS compared to controls and the remaining 19 % displayed hypermethylation in WS. Most of these sites were mapped to gene promoter regions within 5kb of the transcription start site (Figure.S1).

The signature CpG sites were examined using principal component analysis (PCA) (Figure 2A) and hierarchical clustering (Figure 2B) to assess their capacity to separate WS subjects from controls. As seen in Figure 2, the significant CpGs could be used to segregate the discovery cohort of WS from controls. Consistent with the analysis of DNAm at single CpG sites, regional DNAm analysis using a bumphunting approach [29] identified several genomic segments that spanned between 5 and 35 CpG sites overlapping important, previously reported targets of *EZH2*[38] (Table S5). One example of such a genomic segment is the *HOXA* gene cluster, which was also identified as significant at the level of single CpG analysis.

### Validation of the *EZH2* DNAm signature

To test the specificity and sensitivity of the *EZH2* DNAm signature, comprised of 229 CpG sites, we generated median-methylation profiles of controls and WS subjects from the discovery cohort, and classified our independent validation cohort of WS individuals (n = 8) and controls (n = 148) as either 'WS' (positive disease score) or 'not WS' (negative disease score) based on their DNAm profiles using the correlation-based classification model (see Methods). All controls showed DNAm profiles similar to the control profile, had negative disease scores and were classified as "not WS" demonstrating 100% specificity (Figure 3A). Each case in the WS validation cohort clustered with WS and not with controls and generated positive disease scores. Therefore, the validation cohort demonstrated 100% sensitivity (Figure 3A, Table S6). We also tested the ability of the *EZH2* signature to classify DNAm profiles generated from a three-generation family with a segregating *EZH2* variant: GenBank: NM_004456.4; c.466A>G [p.Lys156Glu]. All affected family members clustered with the WS individuals and had positive disease scores (Figure 3A, Table S6).

To further assess the specificity of the *EZH2* signature, we evaluated its performance using a collection of control blood DNAm data extracted from the GEO repository. As there are very limited control data available for the EPIC array, we utilized data from Illumina 450k arrays (n= 718) (Table S7) as well as control 450k array data from our group (n=80) to compare to a subset of the WS-discovery cohort also generated on the 450k array. For this analysis, we defined 161 CpG sites that overlapped the *EZH2* signature on the EPIC and 450k arrays and used the correlation-based classification model (see Methods). As seen in Figure 3B, all 798 control samples had low disease scores for *EZH2* (Table S8), therefore they were predicted as "not WS" (i.e. not to have pathogenic variants in *EZH2*) again demonstrating 100% specificity of the signature (Figure 3B). These results highlight the robustness of the *EZH2* signature, as it overcame many sources of variation such as sex, age, batch, and DNA processing methods contained in the GEO cohorts.

## Classifying models for *EZH2* sequence variants

Using the highly specific and sensitive *EZH2* signature, we tested 19 independent subjects with *EZH2* sequence variants (See Table S9) using the correlation-based model for variant classification (Table S6, Figure 4A). We found that ten subjects had positive disease scores and were therefore classified as "WS" and nine had negative disease scores and were classified as "not WS".

Next, we tested the support vector machine-learning model (SVM), trained on significant CpG sites from the discovery cohorts, on the validation sets of WS and controls. This model generated scores between 0 and 100%, with high scores classified as "WS" and low scores classified as "not WS". We found that it correctly predicted the classification of all WS and control samples with 100% accuracy (Table S10). Then, we used the SVM model on the test cohort of 19 subjects with *EZH2* variants (Table S9, Figure 4B). Ten out of the 19 variants were classified as pathogenic or "WS" (scores between 70-95%) and eight variants were classified as benign or "not-WS" (scores between 0-17%). One subject (described below) had an intermediate SVM score of 49%.

The correlation and SVM models were concordant for predicting the pathogenicity of *EZH2* variants in this testing cohort (Figure 4A and B) with one exception. Both models classified ten of the test cohort samples as pathogenic and 8 as benign.  Those classified as pathogenic included eight with missense variants in *EZH2* (Figure 4, Table S9); five of these were de-identified samples from PreventionGenetics each with an associated clinical diagnosis of WS (PG-55; PG-61; PG-75; PG-87; and PG-45). The other three missense variants  included a clinically affected father -child pair (EX0079 and EX0080, respectively) and one individual (MDL#76455) with an *EZH2* variant: GenBank: NM_004456.4; c.2006G>A [p.Ser669Asn] inherited from a tall but clinically unaffected father (MDL#67485). The other two variants predicted to be pathogenic were copy number variants (CNV) including, a previously published *EZH2* deletion: GenBank: NM_004456.4; *EZH2* (partial [exon20] deletion) (25.42 kb deletion involving *EZH2* and *CUL1*) associated with WS [6] and, an *EZH2* duplication: GenBank: NM_004456.4; _c.2196-2_2211dupAGATACAGCCAGGCTGAT [1]. The latter CNV was identified in an individual diagnosed with WS at birth (S126694). Although this sample had a positive disease score, it did not cluster with the majority of WS samples. Review of the clinical findings for this individual revealed an atypical presentation i.e. more severe ID than most individuals with WS, as well as seizures and contractures, suggesting the possibility of a dual or more complex genetic diagnosis.

The sample for which discordant results were obtained was MDL#67485, the father of MDL#76455. Both father and son were identified to have the same *EZH2* variant, however, the child had a clinical diagnosis of WS while the father presented with tall stature but no other features of WS. The affected son (MDL#76455) had an SVM score of 82 % and a positive disease score of 0.04 using the correlation-based model. The SVM score in the father was in the intermediate range (49%) but he had a negative disease score of -0.12. Considering the discordant predictions for the same variant, we investigated the possibility of somatic mosaicism for the *EZH2* variant in the father's blood-derived genomic DNA. Using quantitative pyrosequencing, we genotyped the *EZH2* variant in both the father and the affected child and found that the percentage of the variant allele was 46% in the blood of the child, but only 38% in the blood of the father suggesting somatic mosaicism.

The eight samples that were classified by both models as benign included five subjects with undiagnosed OGID who inherited an *EZH2* variant: GenBank: NM_004456.4; c.553G>C [p.Asp185His]. None of these individuals had the typical features of WS. Limited family history information was available; in one case the variant was known to be inherited from a phenotypically normal parent (Table S9).

Two subjects with *EZH2 de novo* missense variants and clinical findings atypical for WS were classified as benign using both classification models (Figure 4A and 4B). The subject with the *EZH2* variant: GenBank: NM_004456.4; c.897+5G>A had a height SD +2.0, head circumference, OFC SD +1.5 (age of assessment, 6 years) and moderate intellectual disability with autism spectrum disorder (ASD). This variant had a negative correlation-based disease score (-0.3) and low SVM score of 1% and was therefore classified as benign or "not-WS". The individual with *EZH2* variant: GenBank: NM_004456.4; c.1072C>T [p. Arg358Cys] was 6'3 at 21 years of age with normal intellect. This variant had a negative disease score of -0.16 and an SVM score of 17% and was classified as "not-WS".

Next, we tested an interesting *de novo EZH2* variant identified in an individual who presented with a phenotype characterized by growth failure. This child was born by Cesarean section at 39 weeks gestation for fetal distress. Birth weight was 2055g, length 43 cm and head circumference 33 cm. There was no family history of WS. She had transient neonatal hypoglycemia and hypotonia. At 9 months of age she had a "clover-leaf" shaped skull, large anterior fontanelle, sparse eyebrows, upslanting palpebral fissures and small ears. Development was moderately to severely delayed. By age 6 years, her weight was 9 kg, length 90 cm, and head circumference <3rd centile for age.

The *EZH2* variant: GenBank: NM_004456.4; c.2212G>A [p.Ala738Thr] in this subject (A1646) was predicted to be "not-WS" with an SVM score of 0% and a negative disease score of -0.47. Unsupervised hierarchical clustering of this variant showed that it clustered separately from both controls and from WS individuals but, interestingly, it generated a DNAm profile *opposite* to that of the WS individuals and very different from control individuals (Figure 5A and Figure S2). This suggested that p.Ala738Thr is a GoF variant rather than a LoF variant for *EZH2* which is also consistent with the phenotypic presentation (undergrowth rather than overgrowth). To further assess the putative GoF effect of this variant, a luminescence enzymatic assay was done at BPS Bioscience to test the enzymatic activity of *EZH2* p.Ala738Thr. As shown in Figure 5B, this assay demonstrated increased enzymatic activity of this variant compared to wild-type *EZH2*.

Next, we performed a *de novo* modeling of the post-SET domain of EZH2, building a protein structure including the Ala738 residue and associated proteins. We used the S-Adenosyl Methionine (SAM) and S-Adenosyl Homocysteine (SAH) structures  to obtain the EZH2-SAM and EZH2-SAH complexes , respectively (Figure S3A).We found that the substitution of the Ala 738 residue to Threonine does not significantly change the affinity for SAM (Figure S3B) whereas the substitution of the Ala738 residue to Threonine induces an intermediate SAM/SAH binding mode featuring both the rotation of Gln735 side chain into a SAM-favourable state and a hydrogen-bond network that involves the side chains of Gln735, Ala738Thr and Tyr663, leading to an increased affinity for both cofactors (Figure S3C). Taken together, these data support the hypothesis that this mutant form of EZH2 has a higher affinity for an active intermediate state of the enzyme, leading to the observed increased processivity (i.e. GoF).

## Shared functionality in PRC2 complex genes

Pathogenic sequence variants in, *EZH2*, *SUZ12* and *EED*, the core components of the PRC2 complex, have been associated with three clinically overlapping but distinct syndromes: Weaver, SUZ12-related overgrowth and Cohen-Gibson syndromes, respectively. Therefore, we tested the ability of the *EZH2* signature to predict the pathogenicity of variants in *EED (n=3)* and *SUZ12 (n=4*), in individuals with features that overlap WS and also in an individual who underwent genome sequencing for investigation of ASD (no other clinical information available), who was identified to have a 1.4 Mb 17q11.2 dup including *NF1* [MIM:613113], *SUZ12* and several RefSeq  genes (Table S9). We used both the correlation-based and SVM models to classify these variants. All three subjects with *EED* missense variants showed high SVM scores, between 92% and 96% and had positive disease scores (Figure 6, Tables S6 and S10) suggesting a pathogenic variant. Two subjects with *SUZ12* missense variants (A1765 and EX0066) had high SVM scores (92% and 96%) and positive disease scores. The third subject (EX0067) is the father of EX0066, who presented with mild clinical OGID features including tall stature, prominent forehead, chin crease and normal intellect, and was identified to be mosaic for the variant by PCR based deep sequencing. He was found to have 8.4% mosaicism in blood leukocytes and 27% mosaicism in hair[6]. While the child had a 96% SVM score and a disease score of +0.36, the father had an SVM score of 19% and a disease score of -0.17. The low level of variant mosaicism in blood likely accounts for the negative scores and for the benign classification of this variant in the father.  The fourth subject (M/R728468(2)) with a *SUZ12* variant of unknown significance (VUS) had an SVM score of 5% and a disease score of -0.35. He presented with an atypical phenotype and inherited the variant from a clinically normal father, validating its benign classification. The fifth subject (EX0209) who harbored a duplication including *SUZ12* had an SVM score of 2% and a negative disease score of -0.27 suggesting that the duplication of *SUZ12* is unrelated to the OGID phenotype associated with LoF in SUZ12-related overgrowth syndrome.

## Classification of overgrowth syndromes

Since overgrowth syndromes caused by heterozygous sequence variants in epigenes often share overlapping clinical features, we investigated the DNAm profile generated on the 450k arrays for Sotos syndrome (n=49 [MIM: 117550]), Tatton-Brown Rahman syndrome (n=5 [MIM: 615879]) and susceptibility to ASD (n=10 [MIM: 615032]) caused by pathogenic variants in *NSD1* [MIM: 606681], *DNMT3A* [MIM: 602769] and *CHD8* [MIM: 610528] respectively. [9; 14; 22] The DNAm profiles of these individuals were compared to seven WS individuals (with pathogenic *EZH2* variants) from the discovery cohort, and 80 control samples generated on the 450k. All individuals with pathogenic variants in *NSD1*, *DNMT3A* and *CHD8* received a strongly negative disease score (Figure 7 and Table S11) and were therefore classified as “not WS”.

## Classification of undiagnosed overgrowth syndromes

In order to investigate the potential utility of the *EZH2* signature as a first-tier diagnostic assay, we compared the profiles of 73 methylomes generated in our laboratory using the 450k on blood samples from individuals with OGID that tested negative for targeted sequencing of *NSD1* and *EZH2*. The goal of this analysis was to determine if disease-specific DNAm signatures could be utilized to improve the diagnostic yield in this patient population. Using the *EZH2* signature, we were able to identify two samples that showed a positive disease score of 0.12 and 0.2 (Figure 8, Table S11). These two subjects were clinically diagnosed as WS but targeted testing of *EZH2,* and subsequently *EED,* were negative for both individuals. Since the DNAm profiles for these two subjects clustered with WS individuals, we performed next generation sequencing analysis on a research basis and identified in each subject a *de novo* frameshift variants in

*SUZ12*: GenBank: NM_015355.3; c.1878del [p.Phe626Leufs*7]; and c.1715_1716insCA [p.Leu572Phefs*11]. These two variants were validated by Sanger sequencing as recently reported.[39] The clinical findings in both individuals were consistent with those reported in other individuals with SUZ12-related overgrowth, which has phenotypic overlap with WS, as recently described.[39] These data provide further evidence for the utility of DNAm profiling as a first-tier diagnostic tool, in addition to its previously recognized proficiency as a second-tier tool for VUS classification.[9; 10; 40]

### Functional enrichment of the *EZH2* DNAm signature

Gene-set enrichment analysis was performed using g:Profiler [32] on the 89 genes that overlapped the 229 CpG sites in the *EZH2* DNAm signature. The results demonstrate enrichment for genes with roles in pattern specification processes, skeletal system development, and regulation of morphogenesis such as Homeobox A5, *HOXA5* [MIM: 142952], ALX homeobox 4, *ALX4* [MIM: 605420] and SIX homeobox 2, *SIX2* [MIM: 604994] (Figure S4A, Table S12) (Benjamini-Hochberg corrected *p*-value<0.01). This enrichment in skeletal development and organ morphogenesis pathways reflects the known roles of the PRC2 core complex in cellular lineage (and subsequent tissue) specification, and also reflects some of the cardinal features of WS (i.e. tall stature, advanced osseous maturation, neuronal migration disorders and developmental delay) (Figure S4B), thereby further validating the utility of this signature to elucidate the functional, biological and molecular impact of *EZH2* pathogenic variants.

### Discussion

We have identified a highly sensitive and specific, *EZH2* DNAm signature that can be used to classify missense variants in *EZH2* as pathogenic or benign. Notably, this is the first report of a DNAm signature offering unique insights into GoF sequence variants and for the detection of somatic mosaicism. Further, this signature has utility in classifying sequence variants in two other genes, *EED* and *SUZ12* that encode proteins that participate with EZH2 in the repressive PRC2 complex. Finally, we demonstrated the first-tier diagnostic capability of this signature, based on its ability to predict the presence of pathogenic variants in a PRC2 complex gene (*SUZ12*) in two individuals with undiagnosed OGID syndrome.

In the development of DNAm signatures, an important consideration is the issue of cell type variation. As DNA methylation varies markedly among all cell types, including hematopoietic cells,[41] it is important to account for inter-individual differences in cell types of whole blood samples when analyzing DNAm data from this tissue .[42] Here, we estimated the cell proportions in the discovery cohort using the Houseman method[28] and included these estimates as covariates when identifying *EZH2*-specific signature. This method uses DNAm measured in purified blood cells from a small number of healthy adults to generate cell proportion estimates in mixed cell populations, such as whole blood. We found no statistically significant differences in blood cell type composition between the affected individuals and controls, which aligned with reports of individuals with EZH2-related overgrowth having typical blood cell composition.[43] Future work measuring both complete blood counts and DNAm in the same individuals with WS is needed to confirm the efficacy of the Houseman method in this context.

PRC2 belongs to the Polycomb group (PcG) protein family of chromatin-modifying enzymes that function as repressors of gene expression.[44] In mammalian cells, PRC2 is primarily targeted to the unmethylated CpG islands of inactive developmental genes.[45] PRC2 recruitment and binding to the targeted CpG island is facilitated in part by polycomb-like proteins (PCLs) and JARID2 which link the PRC2 complex to genomic sites enriched in CpG dense regions.[45; 46]

In the *EZH2* LoF (hypomorphic) state, we observed a loss of DNA methylation at CpG sites enriched in promoter regions of developmental genes which can lead to transcriptional changes during critical developmental timepoints resulting in somatic overgrowth characteristic of WS. In the case of the *EZH2* GoF state, we observed a gain of methylation at the same CpG sites which can lead to transcriptional changes during development resulting in growth restriction. Further work is needed to explore the underlying transcriptional dysregulation at the gene promoters overlapping the *EZH2*-specific signature in relevant cell types and critical timepoints during development.

Our results support the position that the DNA methylation changes observed in individuals carrying germline *EZH2* pathogenic variants represent a downstream cascade of events at the molecular level in response to a genetic change. These DNA methylation changes recur across multiple generations if the genetic change is present demonstrating the impact of *EZH2* pathogenic variants on epigenetic programming during embryonic development. Evidence for this hypothesis is provided by our genome-wide DNAm findings in a three-generation family in which the *EZH2* variant segregates from a father to his daughter and her three sons. All family members showed the same *EZH2*-specific epigenotype. This suggests that the same epigenotype was re-established downstream of a dysfunctional PRC2 complex in somatic tissues of each affected family member, in each generation. We have previously shown similar findings in a two generation family where one father and two affected siblings with inherited pathogenic *NSD1* variant all share the same *NSD1*-specific DNA methylation signature. [9]

Constitutional pathogenic variants in *EZH2* are known to cause WS; Most of these are missense variants. Thus, predicting pathogenicity of these variants can present significant challenges, which now can be resolved using the *EZH2* signature. Such classifications are particularly useful for individuals with clinical findings atypical for WS who carry *de novo* missense variants in *EZH2.* The *EZH2* signature, derived from constitutional pathogenic sequence variants, is comprised of differentially methylated CpG sites in WS individuals relative to controls; the majority (> 81%) of these sites are hypomethylated in WS relative to controls, whereas 19% are hypermethylated. This suggests that pathogenic *EZH2* sequence variants cause a failure of promoter CpG methylation at CpG sites critically important for normal growth and development. Support for the functional relevance of the DNAm signature comes from the fact that the most enriched CpG sites and genomic regions overlap *HOX* genes, which are known targets of EZH2[38]. In cancer as well, it has been shown that loss of EZH2 contributes to epigenetic-dependent overexpression of the *HOX* genes[38].

We show that the *EZH2* signature can differentiate the functional effects of missense variants in *EZH2* using two previously validated classification models specifically correlation-based[9; 14; 15] and machine learning.[10; 40; 47] We propose that review of the clinical features of subjects carrying sequence variants in disease genes, such as *EZH2,* combined with the application of several methods to visualize the data in different ways as presented here, can improve the utility of this highly sensitive and specific functional assay for variant pathogenicity classification. We expect that this approach will also be useful for testing the functionality of non-coding variants in disease-associated genes. Discordant results using the two different analytic models were of interest in assessing mosaicism in a father with a sequence variant in *EZH2* who presented with tall stature, normal intellect and no other features of WS. Pyrosequencing studies identified low-level mosaicism in his blood by which is highly relevant for accurate genetic counseling for the family.

In an individual with an *EZH2* missense variant: GenBank: NM_004456.4; c.2212G>A [p.Ala738Thr] who presented with growth restriction rather than an overgrowth phenotype, we considered the possibility of a GoF variant and used three independent approaches to assess this hypothesis. Utilizing the DNAm signature generated using LoF sequence variants in *EZH2*, we identified DNAm alterations at most CpGs observed in the *EZH2* signature but found that these were "opposite in direction" to the DNAm changes in the *EZH2* signature. Further support for a GoF role for this variant was derived from an *in vitro* luminescence assay showing increased enzymatic activity. Finally, protein modeling showed that the Ala738Thr mutated form of EZH2 shows a strong preference for an intermediate SAM/SAH binding state, which helps to explain both the increased processivity observed in vitro, and to corroborate the GoF inferred from the individual-specific methylation profile and the clinical presentation.

It has been shown that methylation of H3K27 by EZH2 requires the presence of two additional proteins: EED and SUZ12. [48] Inactivation of any one of these three protein subunits severely compromises the enzymatic activity of PRC2 and results in the reduction of H3K27me3. [49-51] Not surprisingly, individuals with *EZH2*, *EED* and *SUZ12* pathogenic variants present with overlapping phenotypes, including generalized overgrowth, similar craniofacial features, advanced bone maturation, macrocephaly and variable degrees of intellectual disability. [52] As there are few specific clinical features that distinguish each of these 3 disorders from each other, it is difficult in many of these individuals, for even the most astute clinician, to define specific genomic diagnosis in a particular case. Here we show that the pathogenic sequence variants in these genes that confer similar phenotypes also confer a common DNAm signature that represents the functional effect of PRC2 perturbation during development. As more individuals with sequence variants in *EED* and *SUZ12* are identified, it will become possible to assess whether specific DNAm “sub-signatures” exist for LoF variants in each gene. This will be of great interest to both clinicians and scientist who struggle with elucidating the boundaries between syndromes both molecularly and clinically (lumping versus splitting of syndromes). Although these three conditions currently carry independent names, some would argue that they constitute a phenotypic spectrum that reflects their integrated molecular actions via a shared functional complex.

We have shown that the *EZH2* signature has 100% specificity, in that it does not misclassify as positive any individuals with OGID and pathogenic variants in *NSD1*, *DNMT3A*, or *CHD8*. This is congruent with what we published previously for other OGID signatures such as *NSD1*.[9] We have also demonstrated that a gene-specific DNAm signature can be more broadly applicable if that gene encodes a protein that participates in a functional complex. This is very important for both first-tier diagnostics and for gene discovery. Our work is distinct from that reported for the BAF complex [12] in which the derivation of the signature involved many genes in the complex. In this paper we were able to use the information that the *EZH2* signature also reflected the presence of pathogenic variants in other PRC2 complex genes to efficiently assign a definitive genomic diagnosis to two individuals with features of OGID. In both individuals, a clinical diagnosis of WS was suspected, but targeted sequencing for *EZH2* and *EED* was negative. The fact that DNAm profiles were positive prompted us to arrange next generation sequencing for other genes encoding proteins in the PRC2 complex, leading to the identification of pathogenic sequence variants in *SUZ12*. For the many genes that encode proteins participating in functional complexes, our approach provides a valuable paradigm for first-tier diagnostics that could also play an important role in future novel gene discovery.

There is considerable overlap between germline/constitutional sequence variants observed in WS and the acquired somatic *EZH2* sequence variants observed in myeloid malignancies. Two of the sequence variants present in our WS individuals, p.Arg684Cys and p.Tyr733*, have also been detected as somatically-acquired sequence variants in myeloid malignancies. [53] These two sequence variants were identified constitutionally in seven unrelated individuals in the current series. None of these individuals have developed malignancies, though it is noteworthy that the oldest of these seven individuals is less than 10 years old. Given that myeloid malignancies associated with somatic *EZH2* sequence variants usually present later in life, it will be important to follow these individuals with WS who could be at increased risk of myeloid malignancies not only in childhood, but also over their lifetime. [3] Long-term clinical data for WS will be valuable for time-to-event analysis that estimates the age-specific malignancy risk in these individuals.

In summary, this study demonstrates that pathogenic LoF variants in *EZH2* are associated with a highly sensitive and specific DNAm signature that has significant diagnostic power to classify pathogenic versus benign variants. This study also provides unique finding wherein a DNAm signature has the ability to distinguish GoF from LoF variants, as well as the capability to detect somatic mosaicism of coding *EZH2* variants. Notably we also show that the *EZH2* DNAm signature can positively classify pathogenic sequence variants in two other genes, *EED* and *SUZ12*, encoding proteins in the core PRC2 complex. Finally, we have demonstrated that DNAm signatures for genes that encode proteins in a functional complex can play an important role not only for elucidating molecular pathophysiology and as a tool for first-and second-tier diagnostics, but also for novel paradigms for new gene discovery.

## Acknowledgements

We are grateful to all the families with childhood overgrowth conditions who participated in this research and to the many clinicians who recruited them into the study. We also acknowledge the technical assistance of Youliang Lou and Chunhua Zhao. This work was supported by a Canadian Institutes of Health Research (CIHR) grants to R.W. IGH-155182 and MOP-126054), by CIHR Project Grant PJT-148830 to W.T.G. and by a BCCHR intramural IGAP salary award to W.T.G. Bioinformatic analyses were supported in part by the Canadian Centre for Computational Genomics (C3G), part of the Genome Technology Platform (GTP), funded by Genome Canada through Genome Quebec and Ontario Genomics (ALT, MB), and Genome Canada through Ontario Genomics (ALT, SC, MB, and RW), and the Ontario Brain Institute (OBI). OBI is an independent non-profit corporation, funded partially by the Ontario government. Protein Modeling was supported by Telethon Foundation (grant number GEP13105 to G.T.), the EPIGEN Flagship Project of the Italian National Research Council (to G.T.), the European Research Council (grant number 616441-DISEASEAVATARS to G.T.), and Ricerca Corrente granted by the Italian Ministry of Health (to G.T.). The opinions, results, and conclusions are those of the authors, and no endorsement by the Ontario Brain Institute is intended or should be inferred.

## Web Resources

The URLs for data presented herein are as follows:

OMIM, http://www.omim.org/.

ProteinPaint, https//proteinpaint.stjude.org

AnnotationHub, https://bioconductor.org/packages/release/bioc/
html/AnnotationHub.html

g:Profiler, http://biit.cs.ut.ee/gprofiler/

CADD, https://cadd.gs.washington.edu/snv

GenBank, https://www.ncbi.nlm.nih.gov/genbank/

GEO, https://www.ncbi.nlm.nih.gov/geo/

GREAT, http://great.stanford.edu/public/html/

GROMACS, https://doi.org/10.1016/j.softx.2015.06.001

## Data Availability

Some datasets used in this study are available publicly and may be obtained from gene expression omnibus (GEO) using the following accession numbers: GSE54670, GSE54399, GSE51245, GSE89353, GSE53045, GSE40279, GSE42861, GSE128801, GSE36064, GSE74432, GSE113967 and GSE128801. The remaining datasets are not publicly available due to institutional ethics restrictions.

## Declaration of Interests

The authors declare no competing interests.

## References

1. Tatton-Brown, K., Murray, A., Hanks, S., Douglas, J., Armstrong, R., Banka, S., Bird, L.M., Clericuzio, C.L., Cormier-Daire, V., Cushing, T., et al. (2013). Weaver syndrome and EZH2 mutations: Clarifying the clinical phenotype. American journal of medical genetics Part A 161A, 2972-2980.
2. Gibson, W.T., Hood, R.L., Zhan, S.H., Bulman, D.E., Fejes, A.P., Moore, R., Mungall, A.J., Eydoux, P., Babul-Hirji, R., An, J., et al. (2012). Mutations in EZH2 cause Weaver syndrome. American journal of human genetics 90, 110-118.
3. Tatton-Brown, K., Hanks, S., Ruark, E., Zachariou, A., Duarte Sdel, V., Ramsay, E., Snape, K., Murray, A., Perdeaux, E.R., Seal, S., et al. (2011). Germline mutations in the oncogene EZH2 cause Weaver syndrome and increased human height. Oncotarget 2, 1127-1133.
4. Cao, R., Wang, L., Wang, H., Xia, L., Erdjument-Bromage, H., Tempst, P., Jones, R.S., and Zhang, Y. (2002). Role of histone H3 lysine 27 methylation in Polycomb-group silencing. Science 298, 1039-1043.
5. Cohen, A.S., Tuysuz, B., Shen, Y., Bhalla, S.K., Jones, S.J., and Gibson, W.T. (2015). A novel mutation in EED associated with overgrowth. Journal of human genetics 60, 339-342.
6. Imagawa, E., Higashimoto, K., Sakai, Y., Numakura, C., Okamoto, N., Matsunaga, S., Ryo, A., Sato, Y., Sanefuji, M., Ihara, K., et al. (2017). Mutations in genes encoding polycomb repressive complex 2 subunits cause Weaver syndrome. Human mutation 38, 637-648.
7. Cohen, A.S., and Gibson, W.T. (2016). EED-associated overgrowth in a second male patient. Journal of human genetics 61, 831-834.
8. Lui, J.C., Barnes, K.M., Dong, L., Yue, S., Graber, E., Rapaport, R., Dauber, A., Nilsson, O., and Baron, J. (2018). Ezh2 Mutations Found in the Weaver Overgrowth Syndrome Cause a Partial Loss of H3K27 Histone Methyltransferase Activity. The Journal of clinical endocrinology and metabolism 103, 1470-1478.
9. Choufani, S., Cytrynbaum, C., Chung, B.H., Turinsky, A.L., Grafodatskaya, D., Chen, Y.A., Cohen, A.S., Dupuis, L., Butcher, D.T., Siu, M.T., et al. (2015). NSD1 mutations generate a genome-wide DNA methylation signature. Nature communications 6, 10207.
10. Butcher, D.T., Cytrynbaum, C., Turinsky, A.L., Siu, M.T., Inbar-Feigenberg, M., Mendoza-Londono, R., Chitayat, D., Walker, S., Machado, J., Caluseriu, O., et al. (2017). CHARGE and Kabuki Syndromes: Gene-Specific DNA Methylation Signatures Identify Epigenetic Mechanisms Linking These Clinically Overlapping Conditions. American journal of human genetics 100, 773-788.
11. Grafodatskaya, D., Chung, B.H., Butcher, D.T., Turinsky, A.L., Goodman, S.J., Choufani, S., Chen, Y.A., Lou, Y., Zhao, C., Rajendram, R., et al. (2013). Multilocus loss of DNA methylation in individuals with mutations in the histone H3 Lysine 4 Demethylase KDM5C. BMC Med Genomics 6, 1.
12. Aref-Eshghi, E., Bend, E.G., Hood, R.L., Schenkel, L.C., Carere, D.A., Chakrabarti, R., Nagamani, S.C.S., Cheung, S.W., Campeau, P.M., Prasad, C., et al. (2018). BAFopathies' DNA methylation epi-signatures demonstrate diagnostic utility and functional continuum of Coffin-Siris and Nicolaides-Baraitser syndromes. Nature communications 9, 4885.
13. Aref-Eshghi, E., Rodenhiser, D.I., Schenkel, L.C., Lin, H., Skinner, C., Ainsworth, P., Pare, G., Hood, R.L., Bulman, D.E., Kernohan, K.D., et al. (2018). Genomic DNA Methylation Signatures Enable Concurrent Diagnosis and Clinical Genetic Variant Classification in Neurodevelopmental Syndromes. American journal of human genetics 102, 156-174.
14. Siu, M.T., Butcher, D.T., Turinsky, A.L., Cytrynbaum, C., Stavropoulos, D.J., Walker, S., Caluseriu, O., Carter, M., Lou, Y., Nicolson, R., et al. (2019). Functional DNA methylation signatures for autism

spectrum disorder genomic risk loci: 16p11.2 deletions and CHD8 variants. Clin Epigenetics 11, 103.

15. Chater-Diehl, E., Ejaz, R., Cytrynbaum, C., Siu, M.T., Turinsky, A., Choufani, S., Goodman, S.J., Abdul-Rahman, O., Bedford, M., Dorrani, N., et al. (2019). New insights into DNA methylation signatures: SMARCA2 variants in Nicolaides-Baraitser syndrome. BMC Med Genomics 12, 105.
16. Hanna, G.L., Liu, Y., Isaacs, Y.E., Ayoub, A.M., Torres, J.J., O'Hara, N.B., and Gehring, W.J. (2016). Withdrawn/Depressed Behaviors and Error-Related Brain Activity in Youth With Obsessive-Compulsive Disorder. J Am Acad Child Adolesc Psychiatry 55, 906-913 e902.
17. Accomando, W.P., Wiencke, J.K., Houseman, E.A., Nelson, H.H., and Kelsey, K.T. (2014). Quantitative reconstruction of leukocyte subsets using DNA methylation. Genome Biol 15, R50.
18. Montoya-Williams, D., Quinlan, J., Clukay, C., Rodney, N.C., Kertes, D.A., and Mulligan, C.J. (2018). Associations between maternal prenatal stress, methylation changes in IGF1 and IGF2, and birth weight. J Dev Orig Health Dis 9, 215-222.
19. Friemel, C., Ammerpohl, O., Gutwein, J., Schmutzler, A.G., Caliebe, A., Kautza, M., von Otte, S., Siebert, R., and Bens, S. (2014). Array-based DNA methylation profiling in male infertility reveals allele-specific DNA methylation in PIWIL1 and PIWIL2. Fertil Steril 101, 1097-1103 e1091.
20. Barbosa, M., Joshi, R.S., Garg, P., Martin-Trujillo, A., Patel, N., Jadhav, B., Watson, C.T., Gibson, W., Chetnik, K., Tessereau, C., et al. (2018). Identification of rare de novo epigenetic variations in congenital disorders. Nature communications 9, 2064.
21. Alisch, R.S., Barwick, B.G., Chopra, P., Myrick, L.K., Satten, G.A., Conneely, K.N., and Warren, S.T. (2012). Age-associated DNA methylation in pediatric populations. Genome Res 22, 623-632.
22. Jeffries, A.R., Maroofian, R., Salter, C.G., Chioza, B.A., Cross, H.E., Patton, M.A., Dempster, E., Temple, I.K., Mackay, D.J.G., Rezwan, F.I., et al. (2019). Growth disrupting mutations in epigenetic regulatory molecules are associated with abnormalities of epigenetic aging. Genome Res.
23. Dogan, M.V., Shields, B., Cutrona, C., Gao, L., Gibbons, F.X., Simons, R., Monick, M., Brody, G.H., Tan, K., Beach, S.R., et al. (2014). The effect of smoking on DNA methylation of peripheral blood mononuclear cells from African American women. BMC Genomics 15, 151.
24. Hannum, G., Guinney, J., Zhao, L., Zhang, L., Hughes, G., Sadda, S., Klotzle, B., Bibikova, M., Fan, J.B., Gao, Y., et al. (2013). Genome-wide methylation profiles reveal quantitative views of human aging rates. Mol Cell 49, 359-367.
25. Kular, L., Liu, Y., Ruhrmann, S., Zheleznyakova, G., Marabita, F., Gomez-Cabrero, D., James, T., Ewing, E., Linden, M., Gornikiewicz, B., et al. (2018). DNA methylation as a mediator of HLA-DRB1*15:01 and a protective variant in multiple sclerosis. Nature communications 9, 2397.
26. Bibikova, M., Barnes, B., Tsan, C., Ho, V., Klotzle, B., Le, J.M., Delano, D., Zhang, L., Schroth, G.P., Gunderson, K.L., et al. (2011). High density DNA methylation array with single CpG site resolution. Genomics 98, 288-295.
27. Ritchie, M.E., Phipson, B., Wu, D., Hu, Y., Law, C.W., Shi, W., and Smyth, G.K. (2015). limma powers differential expression analyses for RNA-sequencing and microarray studies. Nucleic acids research 43, e47.
28. Salas, L.A., Koestler, D.C., Butler, R.A., Hansen, H.M., Wiencke, J.K., Kelsey, K.T., and Christensen, B.C. (2018). An optimized library for reference-based deconvolution of whole-blood biospecimens assayed using the Illumina HumanMethylationEPIC BeadArray. Genome Biol 19, 64.
29. Jaffe, A.E., Murakami, P., Lee, H., Leek, J.T., Fallin, M.D., Feinberg, A.P., and Irizarry, R.A. (2012). Bump hunting to identify differentially methylated regions in epigenetic epidemiology studies. Int J Epidemiol 41, 200-209.
30. Li, D., Xie, Z., Pape, M.L., and Dye, T. (2015). An evaluation of statistical methods for DNA methylation microarray data analysis. BMC bioinformatics 16, 217.

31. McLean, C.Y., Bristor, D., Hiller, M., Clarke, S.L., Schaar, B.T., Lowe, C.B., Wenger, A.M., and Bejerano, G. (2010). GREAT improves functional interpretation of cis-regulatory regions. Nat Biotechnol 28, 495-501.
32. Reimand, J., Isserlin, R., Voisin, V., Kucera, M., Tannus-Lopes, C., Rostamianfar, A., Wadi, L., Meyer, M., Wong, J., Xu, C., et al. (2019). Pathway enrichment analysis and visualization of omics data using g:Profiler, GSEA, Cytoscape and EnrichmentMap. Nat Protoc 14, 482-517.
33. Schuttelkopf, A.W., and van Aalten, D.M. (2004). PRODRG: a tool for high-throughput crystallography of protein-ligand complexes. Acta Crystallogr D Biol Crystallogr 60, 1355-1363.
34. Webb, B., and Sali, A. (2016). Comparative Protein Structure Modeling Using MODELLER. Curr Protoc Bioinformatics 54, 5 6 1-5 6 37.
35. Wu, H., Zeng, H., Dong, A., Li, F., He, H., Senisterra, G., Seitova, A., Duan, S., Brown, P.J., Vedadi, M., et al. (2013). Structure of the catalytic domain of EZH2 reveals conformational plasticity in cofactor and substrate binding sites and explains oncogenic mutations. PLoS One 8, e83737.
36. Lindorff-Larsen, K., Piana, S., Palmo, K., Maragakis, P., Klepeis, J.L., Dror, R.O., and Shaw, D.E. (2010). Improved side-chain torsion potentials for the Amber ff99SB protein force field. Proteins 78, 1950-1958.
37. Trott, O., and Olson, A.J. (2010). AutoDock Vina: improving the speed and accuracy of docking with a new scoring function, efficient optimization, and multithreading. J Comput Chem 31, 455-461.
38. Xu, F., Liu, L., Chang, C.K., He, Q., Wu, L.Y., Zhang, Z., Shi, W.H., Guo, J., Zhu, Y., Zhao, Y.S., et al. (2016). Genomic loss of EZH2 leads to epigenetic modifications and overexpression of the HOX gene clusters in myelodysplastic syndrome. Oncotarget 7, 8119-8130.
39. Cyrus, S.S., Cohen, A.S.A., Agbahovbe, R., Avela, K., Yeung, K.S., Chung, B.H.Y., Luk, H.M., Tkachenko, N., Choufani, S., Weksberg, R., et al. (2019). Rare SUZ12 variants commonly cause an overgrowth phenotype. American journal of medical genetics Part C, Seminars in medical genetics 181, 532-547.
40. Aref-Eshghi, E., Bend, E.G., Colaiacovo, S., Caudle, M., Chakrabarti, R., Napier, M., Brick, L., Brady, L., Carere, D.A., Levy, M.A., et al. (2019). Diagnostic Utility of Genome-wide DNA Methylation Testing in Genetically Unsolved Individuals with Suspected Hereditary Conditions. American journal of human genetics 104, 685-700.
41. Reinius, L.E., Acevedo, N., Joerink, M., Pershagen, G., Dahlen, S.E., Greco, D., Soderhall, C., Scheynius, A., and Kere, J. (2012). Differential DNA methylation in purified human blood cells: implications for cell lineage and studies on disease susceptibility. PLoS One 7, e41361.
42. Jaffe, A.E., and Irizarry, R.A. (2014). Accounting for cellular heterogeneity is critical in epigenome-wide association studies. Genome Biol 15, R31.
43. Tatton-Brown, K., and Rahman, N. (1993). EZH2-Related Overgrowth. In GeneReviews((R)), M.P. Adam, H.H. Ardinger, R.A. Pagon, S.E. Wallace, L.J.H. Bean, K. Stephens, andA. Amemiya, eds. (Seattle (WA).
44. Schuettengruber, B., Bourbon, H.M., Di Croce, L., and Cavalli, G. (2017). Genome Regulation by Polycomb and Trithorax: 70 Years and Counting. Cell 171, 34-57.
45. Li, H., Liefke, R., Jiang, J., Kurland, J.V., Tian, W., Deng, P., Zhang, W., He, Q., Patel, D.J., Bulyk, M.L., et al. (2017). Polycomb-like proteins link the PRC2 complex to CpG islands. Nature 549, 287-291.
46. Youmans, D.T., Schmidt, J.C., and Cech, T.R. (2018). Live-cell imaging reveals the dynamics of PRC2 and recruitment to chromatin by SUZ12-associated subunits. Genes Dev 32, 794-805.
47. Capper, D., Jones, D.T.W., Sill, M., Hovestadt, V., Schrimpf, D., Sturm, D., Koelsche, C., Sahm, F., Chavez, L., Reuss, D.E., et al. (2018). DNA methylation-based classification of central nervous system tumours. Nature 555, 469-474.

48. Guglielmelli, P., Biamonte, F., Score, J., Hidalgo-Curtis, C., Cervantes, F., Maffioli, M., Fanelli, T., Ernst, T., Winkelman, N., Jones, A.V., et al. (2011). EZH2 mutational status predicts poor survival in myelofibrosis. Blood 118, 5227-5234.
49. Pasini, D., Bracken, A.P., Jensen, M.R., Lazzerini Denchi, E., and Helin, K. (2004). Suz12 is essential for mouse development and for EZH2 histone methyltransferase activity. EMBO J 23, 4061-4071.
50. Faust, C., Schumacher, A., Holdener, B., and Magnuson, T. (1995). The eed mutation disrupts anterior mesoderm production in mice. Development 121, 273-285.
51. Shen, X., Liu, Y., Hsu, Y.J., Fujiwara, Y., Kim, J., Mao, X., Yuan, G.C., and Orkin, S.H. (2008). EZH1 mediates methylation on histone H3 lysine 27 and complements EZH2 in maintaining stem cell identity and executing pluripotency. Mol Cell 32, 491-502.
52. Imagawa, E., Albuquerque, E.V.A., Isidor, B., Mitsuhashi, S., Mizuguchi, T., Miyatake, S., Takata, A., Miyake, N., Boguszewski, M.C.S., Boguszewski, C.L., et al. (2018). Novel SUZ12 mutations in Weaver-like syndrome. Clinical genetics 94, 461-466.
53. Ernst, T., Chase, A.J., Score, J., Hidalgo-Curtis, C.E., Bryant, C., Jones, A.V., Waghorn, K., Zoi, K., Ross, F.M., Reiter, A., et al. (2010). Inactivating mutations of the histone methyltransferase gene EZH2 in myeloid disorders. Nature genetics 42, 722-726.

## Figure legends

**Figure 1. Comprehensive visualization of *EZH2* sequence variants using ProteinPaint**
Schematic representation of *EZH2* sequence variants included in the study. Each distinct variant in *EZH2* is represented by a disc sized in proportion to the number of samples and filled with the color representing its class based on the legend. Missense variants which constitute the large proportion of variants in *EZH2* are colored in red, nonsense variants in blue and indels in green. Sequence variants are positioned by their amino acid coordinates based on *EZH2* NM_004456.4, hg19. The dotted vertical lines inside the protein delineate the boundaries of coding exons and the filled colors within the protein correspond to known protein domains.

**Figure 2. *EZH2* -specific DNAm signature**
(A) Principal components analysis (PCA) plot and (B) corresponding hierarchical clustering (Eucledian distance metrics) and representative heatmap of 31 samples (n=8 WS; n=23 controls) using the differentially methylated CpG sites comprising the *EZH2*-specific DNAm signature (229 CpG sites). In both A and B, samples labeled with red represent Weaver syndrome, blue samples are controls. On the heat map, yellow indicates high DNAm and blue indicates low DNAm. For the heatmap, data are normalized for visualization (mean=0, variance=1).

**Figure 3. Testing the sensitivity and specificity of the *EZH2*- specific signature**
(A) Plot representing the median-methylation profiles of WS (Y-axis) and controls (X-axis) using the *EZH2* DNAm signature. The dashed line is set to represent the decision boundary for which individuals above the dashed lines have DNAm profiles more similar to *EZH2* signature and below the dashed line have DNAm profiles more similar to controls. A set of independent WS individuals (validation cohort, purple circles, n=8) as well as a WS family (light orange circles, n=5 affected members) with *EZH2* pathogenic variants were classified as “WS” (i.e. all individuals classified as more similar to the *EZH2* signature than controls) indicating high accuracy of the *EZH2* DNAm signature. The specificity of *EZH2* signature was estimated on an independent control validation set of 148 control samples (green crossed boxes); all subjects classified as more similar to controls (specificity 100%). (B) Performance of the *EZH2* signature on data generated on 450k array including overlapping WS subjects from the discovery cohort

n=7 (red circles), controls n=80 (blue squares) and GEO controls n=718 (brown squares) generated on 450k array. All controls had DNAm profiles more similar to the control profile and were therefore classified as “not-WS”. WS-Weaver syndrome.

**Figure 4. Testing the ability of the *EZH2* -specific signature to classify *EZH2* variants**

(A) Plot representing  the median-methylation profiles of WS (Y-axis) and controls (X-axis) using the *EZH2* DNAm signature. A set of independent individuals with *EZH2* sequence variants (pink squares, n=19) were classified using the *EZH2* signature. Of the 19 variants, ten classified as more similar to the *EZH2* DNAm profile than controls. The remaining nine variants classified as more similar to the control profile. (B) Plot representing the  Support Vector machine (SVM) scores (Y-axis). The SVM prediction model was used to predict pathogenicity of *EZH2* variants based on the DNAm signature. All ten variants predicted as pathogenic in (A) had also very high SVM scores > 70% and the remaining nine variants had very low SVM scores < 20% except one variant with an SVM score of 49%. Blue arrow represents sample MDL#67845 (p.Ser669Asn). Orange arrow represents sample S126694 (*EZH2*_c.2196-2_2211dupAGATACAGCCAGGCTGAT). Green arrow represents sample A1646 (p.Ala738Thr). WS-Weaver syndrome.

**Figure 5. Gain of function variant in *EZH2* have opposite DNA methylation profile at the *EZH2* signature**

(A) Heatmap showing the hierarchical clustering of the DNAm profile of WS individuals (n=8, red) with LoF (hypomorphic) variants in *EZH2*, Controls (n=23, blue) and *EZH2* GoF variant (p.Ala738Thr; pink) using the *EZH2* signature. On the heat map, yellow indicates high DNAm and blue indicates low DNAm. The subject with an *EZH2* variant in pink display opposite DNAm profile when compared to WS DNAm profiles. For the heatmap, data are normalized for visualization (mean=0, variance=1). (B) Enzymatic activity of *EZH2* GoF variant using an *in-vitro* luminescence assay. Mutant *EZH2* (p.Ala738Thr) pre-assembled into PRC2 showed increased EZH2-mediated H3K27 methylation activity. WS-Weaver syndrome; GoF-gain of function; LoF-loss of function.

**Figure 6. Testing the utility of the *EZH2* signature in classifying sequence variants in other components of the PRC2 complex**

Using the *EZH2* signature, we compared the DNAm profiles of three subjects with *EED* sequence variants (yellow triangles) and those with *SUZ12* variants (green diamonds) to the DNAm profiles of controls (blue crossed boxes) and *EZH2* pathogenic variants (red circles). All three subjects with pathogenic variants in *EED* had DNAm profiles more similar to the *EZH2* profile than controls. Two subjects with *SUZ12* pathogenic variants also classified with Weaver syndrome and the three remaining *SUZ12* variants showed DNAm profiles more similar to controls.

**Figure 7**. **Classification of subjects with syndromic overgrowth using *EZH2* signature**

Plot representing samples with sequence variants in epigenes associated with other overgrowth syndromes. These included subjects with: *NSD1* pathogenic variants associated with Sotos syndrome (n= 49, GSE74432), *DNMT3A* pathogenic variants associated with Tatton-Brown Rahman syndrome (n=5; GSE128801) and *CHD8* pathogenic variants associated with macrocephaly and susceptibility to autism (n= 10; GSE113967). These data were compared to seven WS subjects from the discovery cohort and five test individuals with pathogenic mutations in *EZH2* which were run on the Illumina 450k. All overgrowth syndrome individuals had DNAm profiles more similar to controls and distinguishable from WS.

**Figure 8**. **Testing the ability of the *EZH2* signature in classifying undiagnosed OGID subjects based on their DNAm profiles**

OGID subjects included in this analysis were previously tested negative for targeted mutations screening in *NSD1* and *EZH2*. Out of the 73 subjects with OGID (brown triangles), we identified that most had DNAm profiles similar to controls (blue squares). Interestingly, we identified two subjects with DNAm profiles more similar to the *EZH2* profile than controls samples. OGID-Overgrowth and Intellectual Disability.

Figure 1

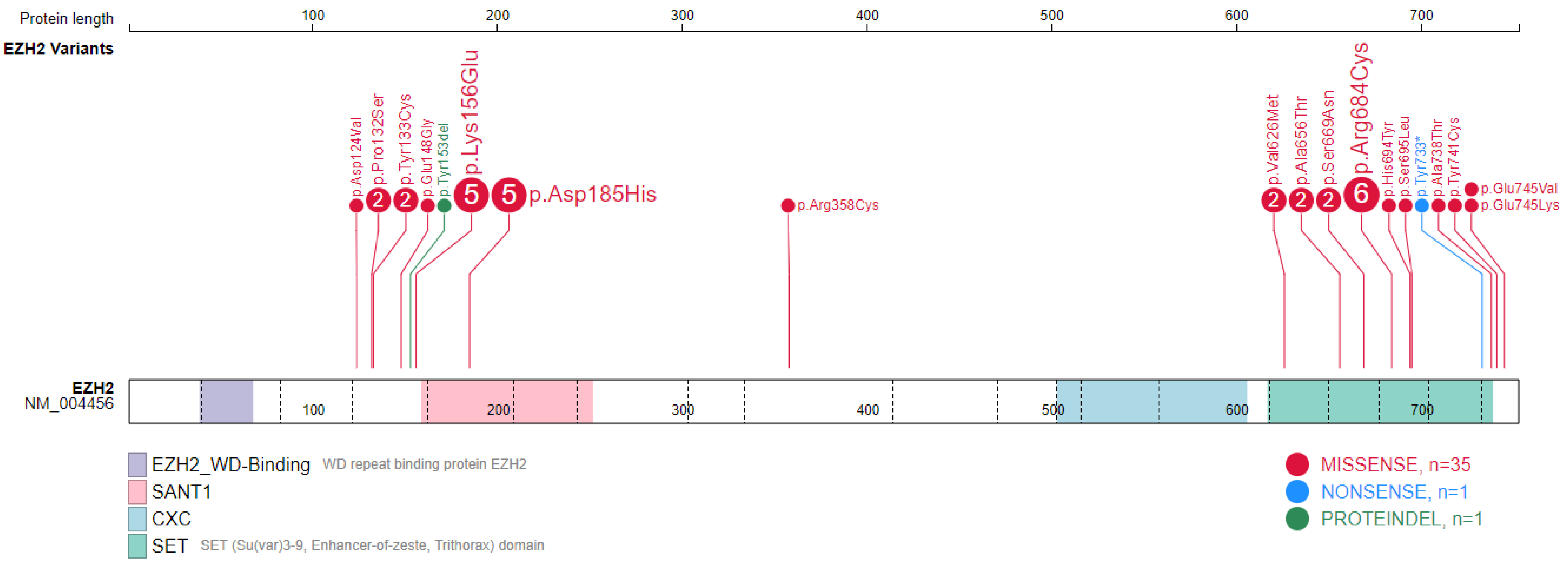

Protein length
100
200
300
400
500
600
700
EZH2 Variants
p.Asp124Val
2
p.Pro132Ser
2
p.Tyr133Cys
p.Glu148Gly
p.Tyr153del
5
p.Lys156Glu
5
p.Asp185His
p.Arg358Cys
2
p.Val626Met
2
p.Ala656Thr
2
p.Ser669Asn
6
p.Arg684Cys
p.His694Tyr
p.Ser695Leu
p.Tyr733*
p.Ala738Thr
p.Tyr741Cys
p.Glu745Val
p.Glu745Lys
EZH2
NM_004456
100
200
300
400
500
600
700
EZH2_WD-Binding
WD repeat binding protein EZH2
SANT1
CXC
SET
SET (Su(var)3-9, Enhancer-of-zeste, Trithorax) domain
MISSENSE, n=35
NONSENSE, n=1
PROTEINDEL, n=1

Figure 2

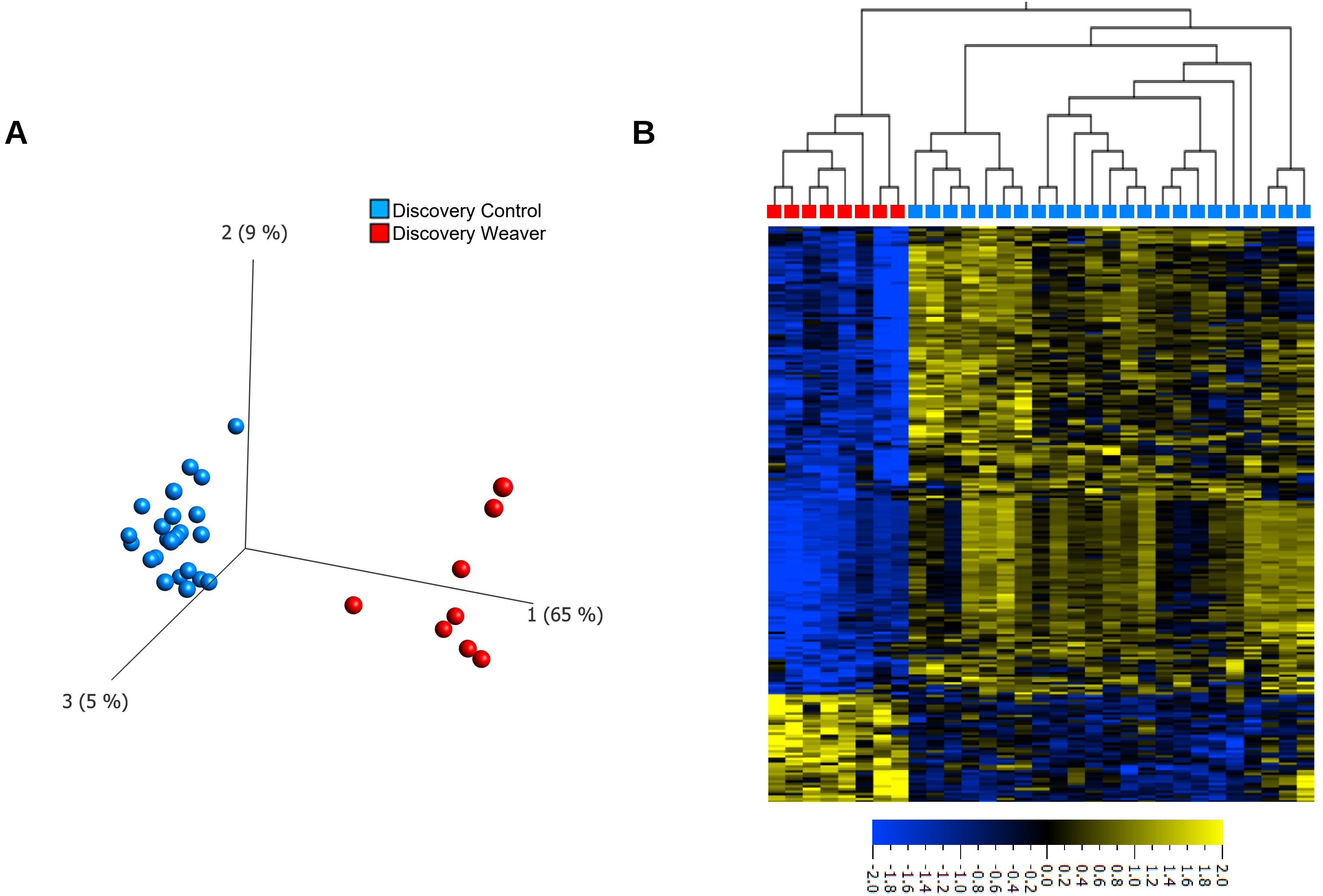
A
🟦 Discovery Control
🟥 Discovery Weaver
2 (9 %)
1 (65 %)
3 (5 %)
B
-2.0
-1.8
-1.6
-1.4
-1.2
-1.0
-0.8
-0.6
-0.4
-0.2
0.0
0.2
0.4
0.6
0.8
1.0
1.2
1.4
1.6
1.8
2.0

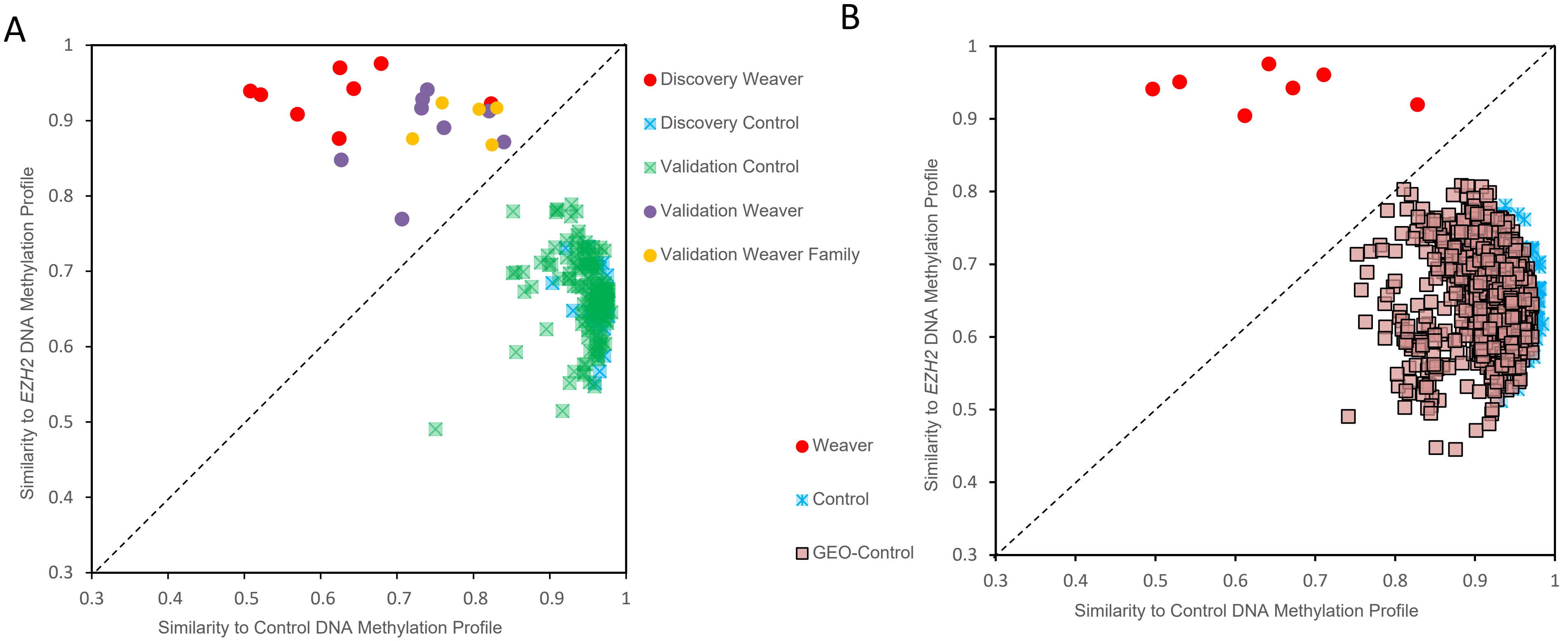
A
1
0.9
0.8
0.7
0.6
0.5
0.4
0.3
0.3
0.4
0.5
0.6
0.7
0.8
0.9
1
Similarity to *EZH2* DNA Methylation Profile
Similarity to Control DNA Methylation Profile
● Discovery Weaver
☒ Discovery Control
☒ Validation Control
● Validation Weaver
● Validation Weaver Family
B
1
0.9
0.8
0.7
0.6
0.5
0.4
0.3
0.3
0.4
0.5
0.6
0.7
0.8
0.9
1
Similarity to *EZH2* DNA Methylation Profile
Similarity to Control DNA Methylation Profile
● Weaver
☒ Control
□ GEO-Control

igure 4

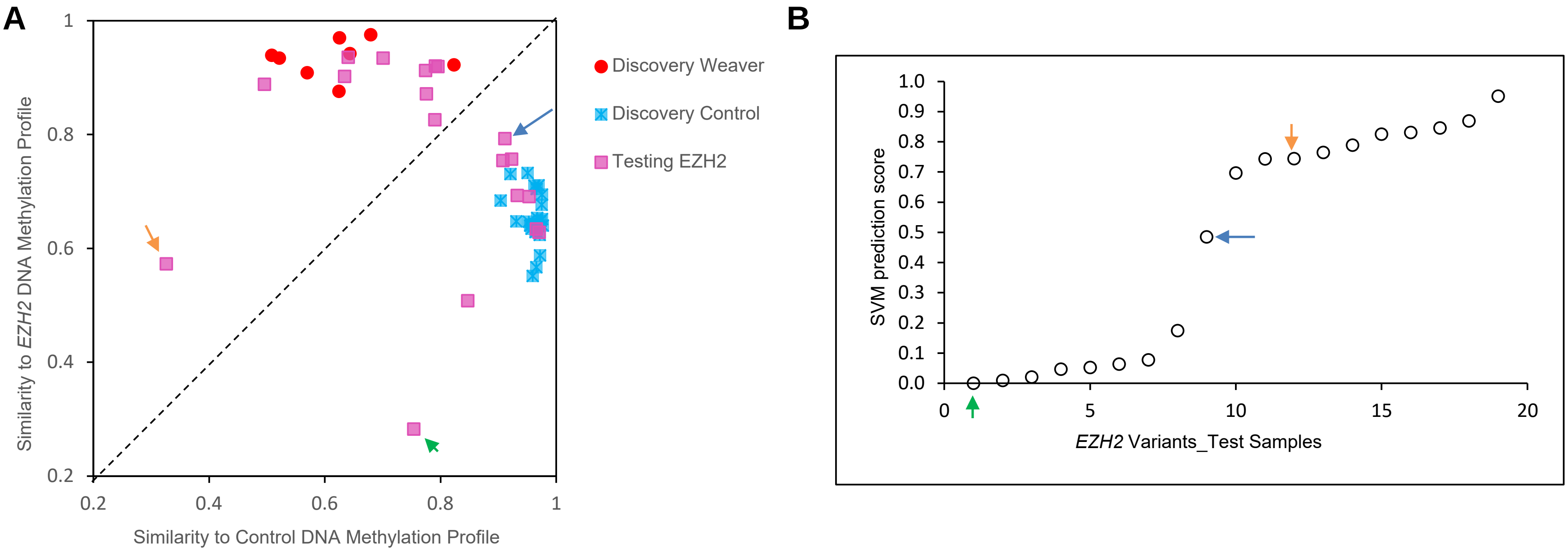
A
1
0.8
0.6
0.4
0.2
0.2
0.4
0.6
0.8
1
Similarity to EZH2 DNA Methylation Profile
Similarity to Control DNA Methylation Profile
● Discovery Weaver
▨ Discovery Control
■ Testing EZH2
B
1.0
0.9
0.8
0.7
0.6
0.5
0.4
0.3
0.2
0.1
0.0
0
5
10
15
20
SVM prediction score
EZH2 Variants_Test Samples

Figure 5

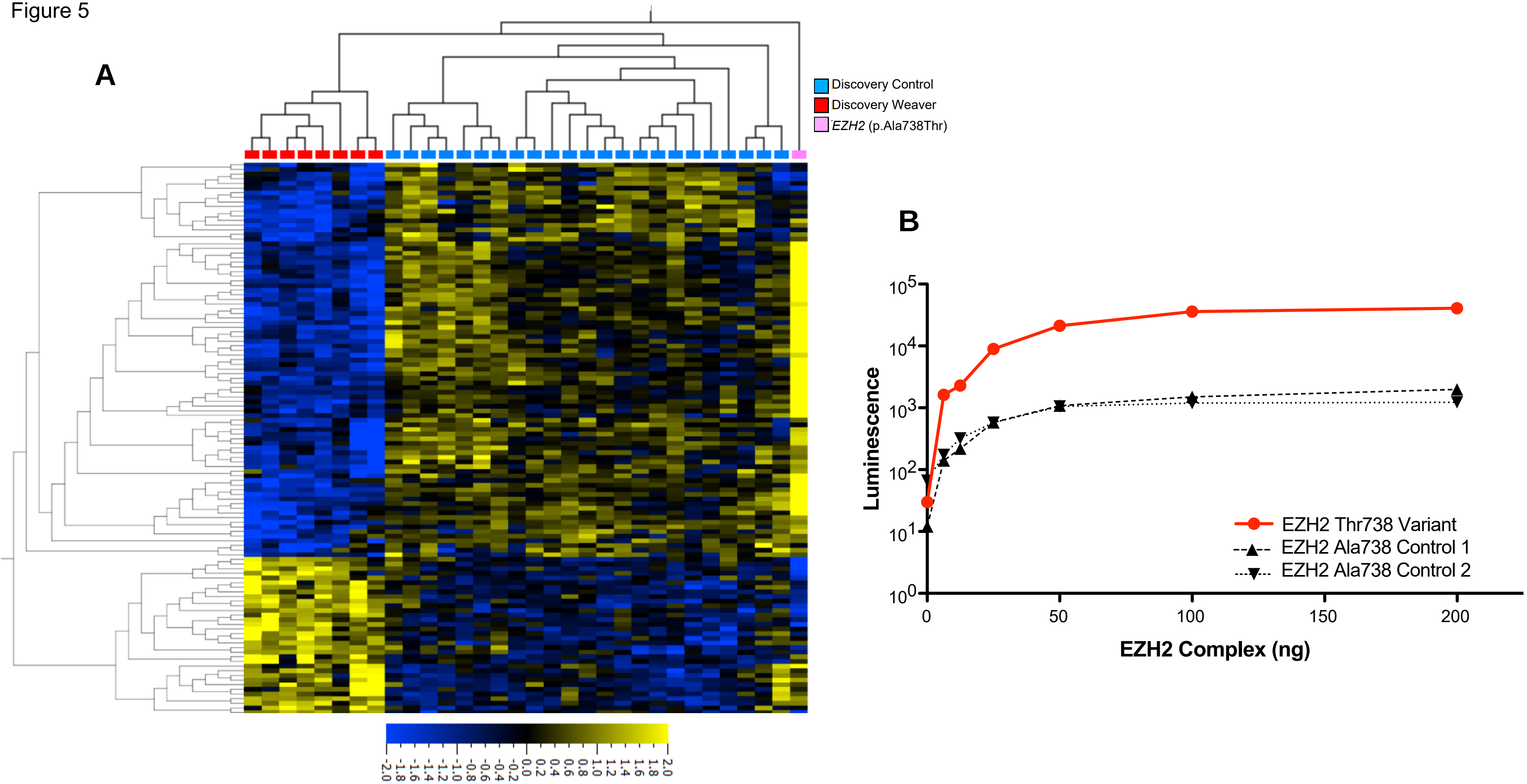
A
Discovery Control
Discovery Weaver
EZH2 (p.Ala738Thr)
-2.0
-1.8
-1.6
-1.4
-1.2
-1.0
-0.8
-0.6
-0.4
-0.2
0.0
0.2
0.4
0.6
0.8
1.0
1.2
1.4
1.6
1.8
2.0
B
Luminescence
10^5
10^4
10^3
10^2
10^1
10^0
0
50
100
150
200
EZH2 Complex (ng)
EZH2 Thr738 Variant
EZH2 Ala738 Control 1
EZH2 Ala738 Control 2

Figure 6

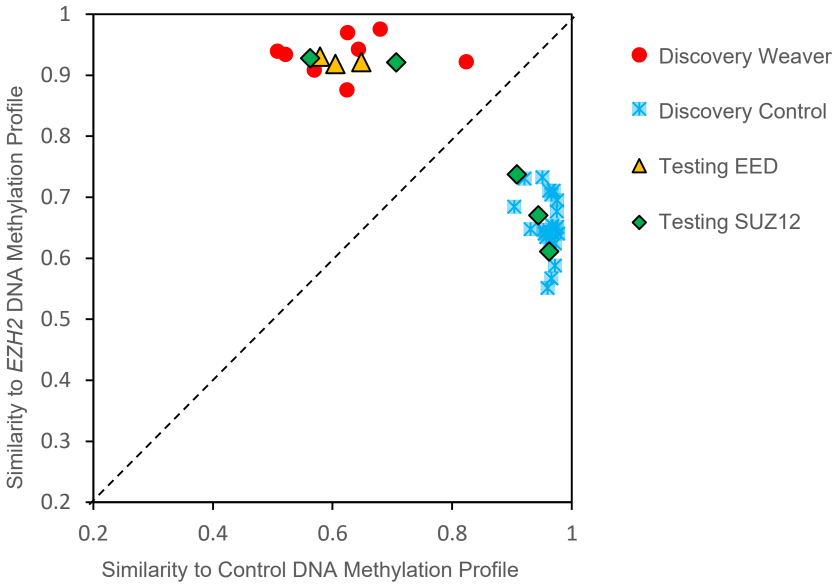
1
0.9
0.8
0.7
0.6
0.5
0.4
0.3
0.2
Similarity to *EZH2* DNA Methylation Profile
0.2
0.4
0.6
0.8
1
Similarity to Control DNA Methylation Profile
Discovery Weaver
Discovery Control
Testing EED
Testing SUZ12

Figure 7

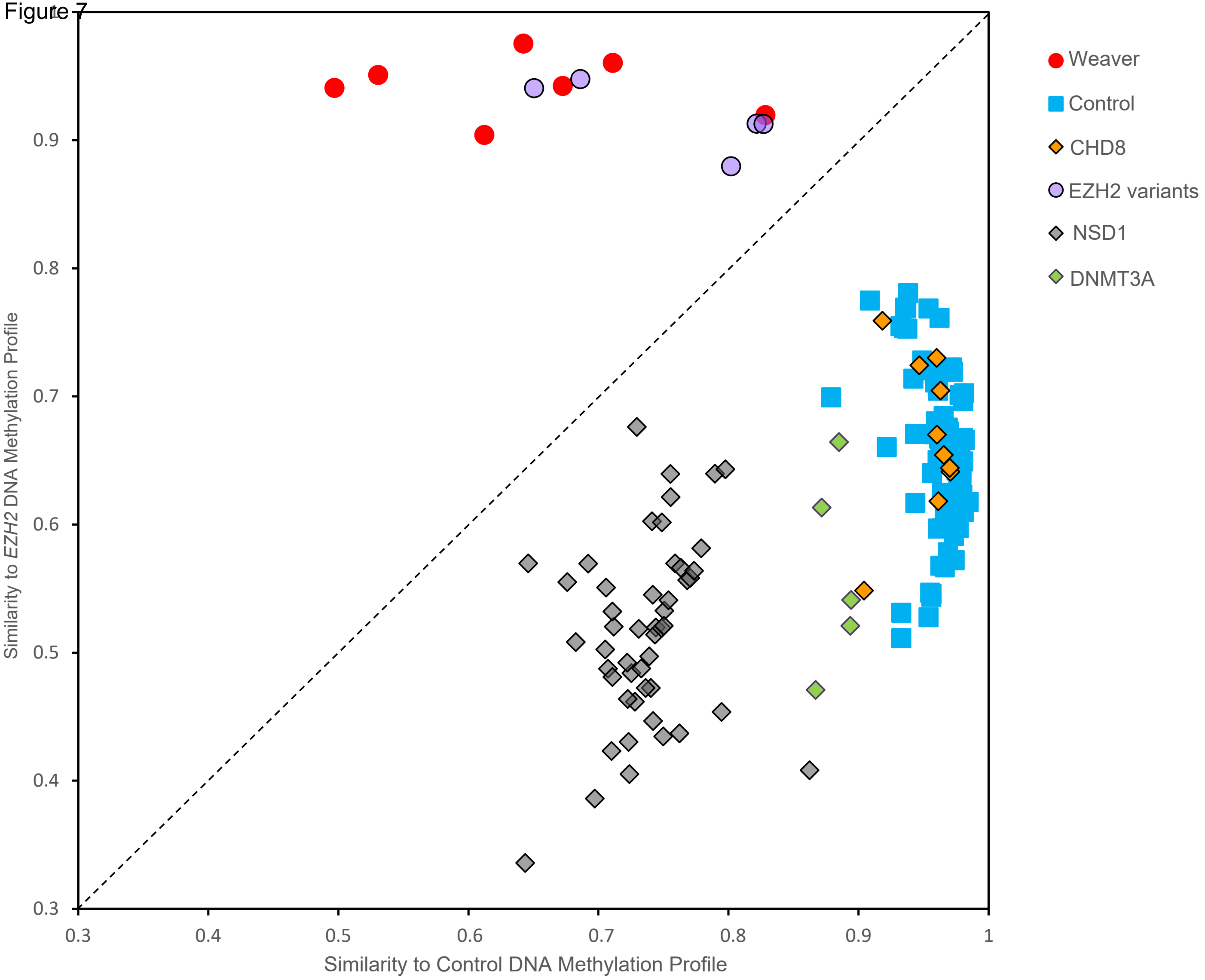
1
0.9
0.8
0.7
0.6
0.5
0.4
0.3
Similarity to *EZH2* DNA Methylation Profile
0.3
0.4
0.5
0.6
0.7
0.8
0.9
1
Similarity to Control DNA Methylation Profile
Weaver
Control
CHD8
EZH2 variants
NSD1
DNMT3A

Figure 8

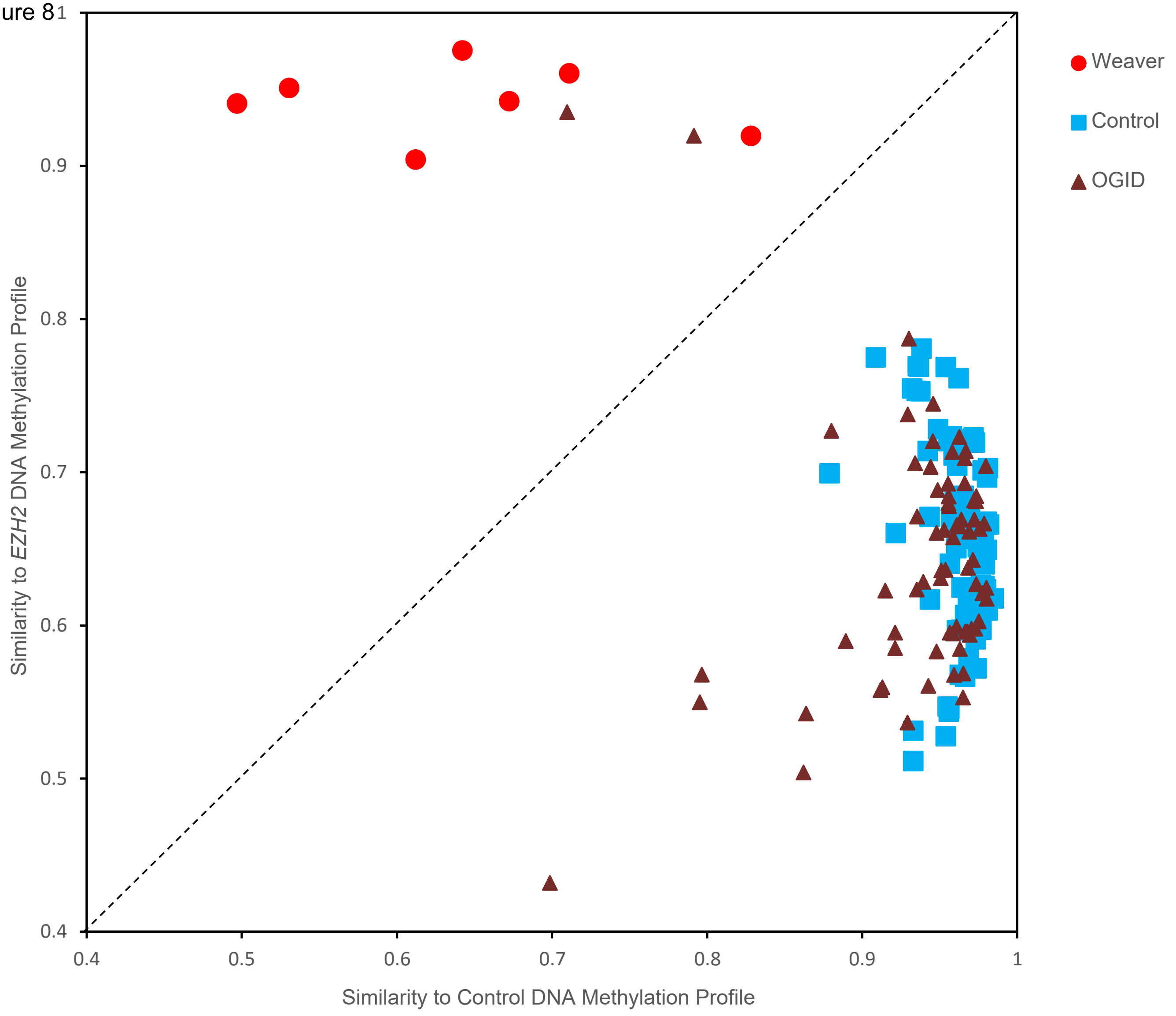

1
0.9
0.8
0.7
0.6
0.5
0.4
0.4
0.5
0.6
0.7
0.8
0.9
1
Similarity to *EZH2* DNA Methylation Profile
Similarity to Control DNA Methylation Profile
● Weaver
■ Control
▲ OGID

Supplemental Tables

Supplemental Figures

# AJHG DECLARATION OF INTERESTS POLICY

Transparency is essential for a reader’s trust in the scientific process and for the credibility of published articles. At AJHG, we feel that disclosure of competing interests is a critical aspect of transparency. Therefore, we ask that all authors disclose any financial or other interests related to the submitted work that (1) could affect or have the perception of affecting the author’s objectivity, or (2) could influence or have the perception of influencing the content of the article, in a “Declaration of Interests” section.

***What types of articles does this apply to?***

We ask that you disclose competing interests for all submitted content, including research articles as well as front matter (e.g., Reviews, Previews, etc.) by completing and submitting the “Declaration of Interests” form below. We also ask that you include a “Declaration of Interests” section in the text of all research articles even if there are no interests declared. For front matter, we ask you to include a “Declaration of Interests” section only when you have information to declare.

***What should I disclose?***

We ask that you and all authors disclose any personal financial interests (examples include stocks or shares in companies with interests related to the submitted work or consulting fees from companies that could have interests related to the work), professional affiliations, advisory positions, board memberships, or patent holdings that are related to the subject matter of the contribution. As a guideline, you need to declare an interest for (1) any affiliation associated with a payment or financial benefit exceeding $10,000 p.a. or 5% ownership of a company or (2) research funding by a company with related interests. You do not need to disclose diversified mutual funds, 401ks, or investment trusts.

***Where do I declare competing interests?***

Competing interests should be disclosed on the “Declaration of Interests” form as well as in the last section of the manuscript before the “References” section, under the heading “Declaration of Interests”. This section should include financial or other competing interests as well as affiliations that are not included in the author list. Examples of “Declaration of Interests” language include:

> “AUTHOR is an employee and shareholder of COMPANY.”
> “AUTHOR is a founder of COMPANY and a member of its scientific advisory board.”

*NOTE:* Primary affiliations should be included on the title page of the manuscript with the author list and do not need to be included in the “Declaration of Interests” section. Funding sources should be included in the “Acknowledgments” section and also do not need to be included in the “Declaration of Interests” section. (A small number of front-matter article types do not include an “Acknowledgments” section. For these articles, reporting of funding sources is not required.)

***What if there are no competing interests to declare?***

For *research* articles, if you have no competing interests to declare, please note that in a “Declaration of Interests” section with the following wording:

> “The authors declare no competing interests.”

*Front-matter* articles do not need to include this section when there are no competing interests to declare.

# AJHG DECLARATION OF INTERESTS FORM

If submitting materials via Editorial Manager, please complete this form and upload with your final submission. Otherwise, please e-mail as an attachment to the editor handling your manuscript.

***Please complete each section of the form and insert any necessary "Declaration of Interest" statement in the text box at the end of the form. A matching statement should be included in a "Declaration of Interest" section in the manuscript.***

## ***Institutional Affiliations***

We ask that you list the current institutional affiliations of all authors, including academic, corporate, and industrial, on the title page of the manuscript. ***Please select one of the following:***

◉ All affiliations are listed on the title page of the manuscript.

○ I or other authors have additional affiliations that we have noted in the "Declaration of Interests" section of the manuscript and on this form below.

## ***Funding Sources***

We ask that you disclose all funding sources for the research described in this work. ***Please confirm the following:***

◉ All funding sources for this study are listed in the "Acknowledgments" section of the manuscript.*

*A small number of front-matter article types do not include an "Acknowledgments" section. For these, reporting funding sources is not required.

## ***Competing Financial Interests***

We ask that authors disclose any financial interests, including financial holdings, professional affiliations, advisory positions, board memberships, receipt of consulting fees etc., that:

(1) could affect or have the perception of affecting the author's objectivity, *or*
(2) could influence or have the perception of influencing the content of the article.

***Please select one of the following:***

◉ The authors have no financial interests to declare.

○ I or other authors have noted any financial interests in the "Declaration of Interests" section of the manuscript and on this form below.

***Advisory/Management and Consulting Positions***

We ask that authors disclose any position, be it a member of a Board or Advisory Committee or a paid consultant, that they have been involved with that is related to this study. ***Please select one of the following:***

● The authors have no positions to declare.

○ I or other authors have management/advisory or consulting relationships noted in the "Declaration of Interests" section of the manuscript and on this form below.

***Patents***

We ask that you disclose any patents related to this work by any of the authors or their institutions. ***Please select one of the following:***

● The authors have no related patents to declare.

○ I or one of my authors have a patent related to this work, which is noted in the "Declaration of Interests" section of the manuscript and on this form below.

***Please insert any "Declaration of Interests" statement in this space.*** This exact text should also be included in the "Declaration of Interests" section of the manuscript. If no authors have a competing interest, please insert the text, "The authors declare no competing interests."

The authors declare no competing interests

**On behalf of all authors, I declare that I have disclosed all competing interests related to this work. If any exist, they have been included in the "Declaration of Interests" section of the manuscript.**

**Name:** Sanaa Choufani

**Manuscript Number (if available):** AJHG-D-19-00804